

# THREE DIMENSIONAL ELASTIC BEAM FRAMES: RIGID JOINT CONDITIONS IN VARIATIONAL AND DIFFERENTIAL FORMULATION

GREGORY BERKOLAIKO AND MAHMOOD ETTEHAD

ABSTRACT. We consider three-dimensional elastic frames constructed out of Euler–Bernoulli beams and describe a simple process of generating joint conditions out of the geometric description of the frame. The corresponding differential operator is shown to be self-adjoint. In the special case of planar frames, the operator decomposes into a direct sum of two operators, one coupling out-of-plane displacement to angular (torsional) displacement and the other coupling in-plane displacement with axial displacement (compression).

Detailed analysis of two examples is presented. We actively exploit the symmetry present in the examples and decompose the operator by restricting it onto reducing subspaces corresponding to irreducible representations of the symmetry group. These “quotient” operators are shown to capture particular oscillation modes of the frame.

## 1. INTRODUCTION

Mathematical modeling of vibration of structures made of joined together beams is a topic of natural interest for engineering research and, more recently, for mathematicians working on differential equations defined on metric graphs. Each beam is described by an Euler–Bernoulli energy functional<sup>1</sup> which involves four degrees of freedom for every infinitesimal element along the beam: lateral displacement (2 degrees of freedom), axial displacement, and angular displacement, see Figure 1 for schematic representation of these degrees of freedom. At a joint, these four functions, supported on the beams involved, must be related via matching conditions that take into account the physics of the joint. The question of describing correct matching conditions is of central importance. So far, most of the engineering literature has been dealing with planar structures (see [38, 36, 42, 20, 48] and references therein) and a recent breakthrough into 3 dimensions has been restricted to rectangular structures [37]. In mathematical literature, in addition to the planarity assumption, a further restriction has been imposed by considering out-of-plane displacements alone (see [12, 7, 40, 23, 17]). As we will see in this paper (and as observed in the engineering literature from the start), this is a significant departure from the mechanical model, since out-of-plane displacements are coupled to angular displacement in all non-trivial structures.

In this paper we focus mostly on studying the rigid joint, a joint where relative angles of participating beams remain constant throughout the motion. We put forward a simple, general and compact description of the matching conditions at the rigid joint (and some of its variants), both for the Lagrangian and Hamiltonian formulations. Mathematically speaking, we describe the closed symmetric sesquilinear form associated with the model as well as the corresponding self-adjoint operator. The results are formulated for a general 3-dimensional structure; in the planar case the Hamiltonian decomposes into a direct sum involving two pairs of coupled degrees of freedom:

---

<sup>1</sup>Or, allowing for more degrees of freedom, by a Timoshenko functional. We will restrict our attention to Euler–Bernoulli theory here.

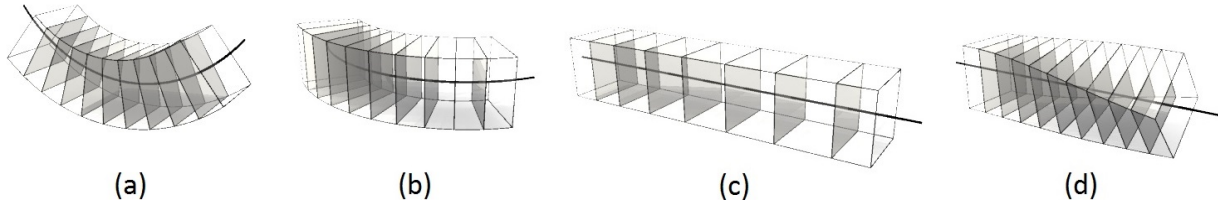


FIGURE 1. Degrees of freedom associated to Euler-Bernoulli beam, (a,b) lateral displacements, (c) axial displacement, and (d) angular displacement.

out-of-plane displacement and angular displacement on one side, in-plane and axial displacements on the other.

To illustrate our results we present two examples, one planar structure and one 3-dimensional structure (“antenna tower”). In the latter example, a significant role is played by the symmetry. We decompose the Hamiltonian operator by restricting it onto reducing subspaces corresponding to irreducible representations of the symmetry group. Numerical simulations of the entire structure are used to illustrate the corresponding decomposition of the vibrational spectrum of the tower.

While maintaining mathematical rigor, we made every effort to highlight the practical aspects of every theorem. Some technicalities are deferred to the Appendix. When presenting results of numerical simulations, we compared the results of direct finite element computations (see, for instance, [1] for analysis of the method on network structures carrying a scalar second order equation) with the results of the method based on characteristic (or secular) equation [50, 51, 49] (also known as “dynamic stiffness matrix method”). In Section 6 we present a partial list of directions for further mathematical investigations together with additional references.

## 2. ELASTICITY OF BEAMS AND BEAM FRAMES

Throughout the manuscript,  $\{\vec{E}_1, \vec{E}_2, \vec{E}_3\}$  will denote the fixed orthonormal basis which spans the physical three dimensional Euclidean space in which the beam frame is embedded.

**2.1. Deformation of an Euler–Bernoulli beam and rigid joint conditions.** According to the Euler–Bernoulli hypothesis, which states that “plane sections remain plane”, the geometry of the spatial beam is described by the centroid line<sup>2</sup> and a family of the cross-sections orthogonal to it. We assume the cross-section of the beam is arbitrary but unchanged along the axis and that the beam is straight in its undeformed configuration. In this case, each undeformed beam is described by an orthonormal basis  $\{\vec{i}, \vec{j}, \vec{k}\}$ , called the cross-section basis or the material basis. The base vector  $\vec{i}$  is directed along the centroid line and the vectors  $\vec{j}$  and  $\vec{k}$  are directed along the principal axes of inertia of the cross-section. The basis is assumed to be right-handed, i.e.  $\vec{i} = \vec{j} \times \vec{k}$ . The choice of orientation, implicit in the choice of the overall sign, is arbitrary but fixed. The deformed configuration of the beam can be fully described by the displacement vector  $\vec{g}(x)$  of the centroid line along with the family of orthonormal bases  $\{\vec{i}(x), \vec{j}(x), \vec{k}(x)\}$  which describe the orientation of the cross sections. Here  $x$  represents the arc-length coordinate along the centroid of the reference (undeformed) configuration, see Figure 2.

Since the Euler–Bernoulli cross sections remain orthogonal to the centroid line, the above parameterization has redundancy (assuming the centroid remains smooth). In what follows we will

<sup>2</sup>The term “centroid” indicates that this line is the locus of the centers of mass of the cross-sections.

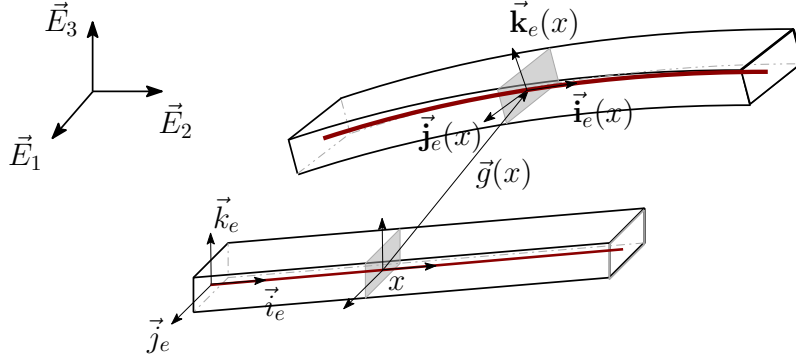


FIGURE 2. Local coordinates of a beam in its initial and deformed configurations.

describe alternative representations of the deformed configuration, finally removing all redundancy in Theorem 3.1.

The relationship between the cross-section basis in the reference and the deformed configurations can be expressed as

$$\vec{i}(x) = \mathcal{R}(x)\vec{i}, \quad \vec{j}(x) = \mathcal{R}(x)\vec{j}, \quad \vec{k}(x) = \mathcal{R}(x)\vec{k} \quad (1)$$

where the **rotation transformation**  $\mathcal{R}(x)$  is an element of  $SO(3)$ , the Lie group of proper orthogonal linear transformations.

Consider now several beams, labeled  $e_1, \dots, e_n$  meeting at a joint. The joint is rigid if it moves as a whole, preserving both the connection and the relative angles of all incident beams<sup>3</sup>. Figure 3 shows an example of a rigid joint. Mathematically, the deformed configuration of a joint is described by its displacement and rotation which are obtained as the (coinciding!) limits of the corresponding vectors along any beam attached to the joint [29, 30].



FIGURE 3. Connection of beams by rigid joints (source).

**Definition 1.** A joint  $\mathbf{v}$  with  $n$  incident beams  $\{e_j\}_{j=1}^n$  is called **rigid**, if the displacement and rotation on beams  $e_j$  satisfy

$$\vec{g}_{e_1}(\mathbf{v}) = \dots = \vec{g}_{e_n}(\mathbf{v}), \quad (2a)$$

$$\mathcal{R}_{e_1}(\mathbf{v}) = \dots = \mathcal{R}_{e_n}(\mathbf{v}), \quad (2b)$$

<sup>3</sup>In engineering, this is called “fully rigid joint” to distinguish from other situations when beams may experience limited bending at the attachment points

where

$$\vec{g}_{e_j}(\mathbf{v}) = \lim_{x \rightarrow \mathbf{v}} \vec{g}_{e_j}(x), \quad \mathcal{R}_{e_j}(\mathbf{v}) = \lim_{x \rightarrow \mathbf{v}} \mathcal{R}_{e_j}(x). \quad (3)$$

We call a rigid joint **free** if it has no further restrictions imposed on it.

Note that the definition assumes that the limits in (3) exist; this will require a certain degree of smoothness of the functions defined on the beams, see the discussion preceding (8) below.

**2.2. Euler–Bernoulli energy functional.** We now represent the centroid displacement vector  $\vec{g}(x)$  in the reference basis of the undeformed beam,

$$\vec{g}(x) =: u(x)\vec{i} + w(x)\vec{j} + v(x)\vec{k}. \quad (4)$$

The component  $u(x)$  is called the **axial displacement** and  $w(x)$  and  $v(x)$  are **lateral displacements**. We also introduce the **in-axis angular displacement**<sup>4</sup>

$$\eta(x) := \vec{j}(x) \cdot \vec{k} = \mathcal{R}(x)\vec{j} \cdot \vec{k}. \quad (5)$$

In the context of the kinematic Bernoulli assumptions for the beam, no pre-stress or external force, the total strain energy of small deformations of the beam can be expressed as (see, e.g. [16, section 5.3.4] or [21])

$$\mathcal{U}^{(e)} := \int_e \left( a(x)|v''(x)|^2 + b(x)|w''(x)|^2 + c(x)|u'(x)|^2 + d(x)|\eta'(x)|^2 \right) dx. \quad (6)$$

The integration here is over the beam  $e$ , parameterized by the arc-length  $x \in [0, \ell]$ . Interpretation of the parameters in the energy functional are as follows: the parameter  $a(x)$  represents the bending stiffness about the local axis  $\vec{j}$  at point  $x$  along the beam,  $b(x)$  represents the bending stiffness about the local axis  $\vec{k}$ ,  $c(x)$  represents the axial stiffness in the direction of  $\vec{i}$ , and, finally,  $d(x)$  represents the angular displacement stiffness in the direction of  $\vec{i}$ . Throughout the rest of the manuscript we assume each beam in our frame is homogeneous in the axial direction and hence

$$a(x) \equiv a_e, \quad b(x) \equiv b_e, \quad c(x) \equiv c_e, \quad \text{and} \quad d(x) \equiv d_e \quad (7)$$

are real, positive constants. Extension of all results to variable stiffness is straightforward.

Some remarks are in order. First, the separation of lateral displacements  $v(x)$  and  $w(x)$  in the energy functional is a consequence of choosing the axes  $\vec{j}$  and  $\vec{k}$  to coincide with the principal axes of inertia of the cross-section. Second, as a consequence of Euler–Bernoulli hypothesis, only one component of  $\mathcal{R}(x)$  participates in the strain energy. The other components are derived quantities which will be expressed in terms of the centroid displacement  $\vec{g}(x)$  when we describe  $\mathcal{R}(x)$  via linearized rotation vector.

**2.3. Beam frames with rigid joints.** A **beam frame** is a collection of beams connected at joints. We will describe a beam frame as a geometric graph  $\Gamma = (V, E)$ , where  $V$  denotes the set of vertices and  $E$  the set of edges. The vertices  $\mathbf{v} \in V$  correspond to joints and edges  $e \in E$  are the beams. Each edge  $e$  is a collection of the following information: origin and terminus vertices  $\mathbf{v}_e^o, \mathbf{v}_e^t \in V$ , length  $\ell_e$  and the local basis  $\{\vec{i}_e, \vec{j}_e, \vec{k}_e\}$ . Describing the vertices  $V$  as points in  $\mathbb{R}^3$  also fixes the length  $\ell_e$  and the axial direction  $\vec{i}_e$  (from origin to terminus); the choice of  $\vec{j}_e$  in the plane orthogonal to  $\vec{i}_e$  still needs to be specified externally.

<sup>4</sup>Alternative terminology includes names such as “longitudinal deflection” for  $u(x)$ , “transverse deflection” for  $(w(x), v(x))$  and “torsional deflection” for  $\eta(x)$ .

The distinction between origin and terminus, and thus the direction of  $\vec{i}_e$  is unimportant in analysis but should be fixed for consistency. It is important to use the same beam basis when writing out joint conditions at both ends of the beam. We will use the **signed incidence indicator**  $s_{\mathbf{v}}^e$  which is defined to be 1 when  $\mathbf{v}$  is the origin of  $e$ ,  $-1$  if it is the terminus of  $e$  and 0 otherwise. We will also write  $e \sim \mathbf{v}$  when  $\mathbf{v}$  is either the origin or the terminus of  $e$ .

The precise meaning of the terms like  $\vec{g}_e(\mathbf{v})$  and  $\mathcal{R}_{e_1}(\mathbf{v})$  in equations (2) depends on whether  $\mathbf{v}$  is the origin or the terminus of  $e$ . In the sequel,  $\vec{g}_e$  will be sufficiently smooth (at least Sobolev  $H^1$ ) vector-function defined on the open interval  $(0, \ell_e)$  and

$$\vec{g}_e(\mathbf{v}_e^o) := \lim_{x \rightarrow 0} \vec{g}_e(x), \quad \vec{g}_e(\mathbf{v}_e^t) := \lim_{x \rightarrow \ell_e} \vec{g}_e(x), \quad (8)$$

and similarly for  $\eta_e$ .

Finally, the strain energy of the beam frame (assuming no vertex energy) is a sum of energies of the individual beams,

$$\mathcal{U}^{(\Gamma)} := \sum_{e \in E} \mathcal{U}^{(e)} = \sum_{e \in E} \int_e \left( a_e |v_e''(x)|^2 + b_e |w_e''(x)|^2 + c_e |u_e'(x)|^2 + d_e |\eta_e'(x)|^2 \right) dx. \quad (9)$$

The interaction between different beams affects the energy via constraints (2) which are imposed on the domain of  $\mathcal{U}^{(\Gamma)}$ . We make this mathematically precise in the next section.

We stress that in the present paper we assume that joints are rigid and we focus primarily on the free rigid joints. Other common cases include pinned (displacement is zero) and clamped (displacement and rotation are zero) rigid joints. These extensions are briefly discussed in section 4.3. Other flavor of joint conditions can happen in real world application and mathematical modeling, see, for example, [45, 38]. Pathways for extending the current framework to more general joint conditions are discussed in Remark 4.6.

### 3. ENERGY FORM AND ITS CORRESPONDING SELF-ADJOINT DIFFERENTIAL OPERATOR

**3.1. Primary matching conditions: the form domain.** We now give a formal mathematical description of the Euler–Bernoulli strain energy form.

**Theorem 3.1.** *The energy functional (9) of the beam frame with free rigid joints is the quadratic form corresponding to the positive closed sesquilinear form*

$$h \left[ \tilde{\Psi}, \Psi \right] := \sum_{e \in E} \int_e \left( a_e \overline{\tilde{v}}_e'' v_e'' + b_e \overline{\tilde{w}}_e'' w_e'' + c_e \overline{\tilde{u}}_e' u_e' + d_e \overline{\tilde{\eta}}_e' \eta_e' \right) dx, \quad (10)$$

*densely defined on the Hilbert space*

$$L^2(\Gamma) := \bigoplus_{e \in E} L^2(e) \oplus \bigoplus_{e \in E} L^2(e) \oplus \bigoplus_{e \in E} L^2(e) \oplus \bigoplus_{e \in E} L^2(e), \quad (11)$$

*with the domain of  $h$  consisting of the vectors*

$$\Psi := (v, w, u, \eta)^T \in \bigoplus_{e \in E} H^2(e) \oplus \bigoplus_{e \in E} H^2(e) \oplus \bigoplus_{e \in E} H^1(e) \oplus \bigoplus_{e \in E} H^1(e) =: \tilde{\mathfrak{h}}(\Gamma) \quad (12)$$

*that satisfy, at every vertex  $\mathbf{v} \in V$ , the **free rigid joint** conditions*

(i) *continuity of displacement: for all  $e, e' \sim \mathbf{v}$ ,*

$$u_e \vec{i}_e + w_e \vec{j}_e + v_e \vec{k}_e = u_{e'} \vec{i}_{e'} + w_{e'} \vec{j}_{e'} + v_{e'} \vec{k}_{e'}, \quad (13)$$

(ii) *continuity of rotation: for all  $e, e' \sim \mathbf{v}$ ,*

$$\eta_e \vec{i}_e - v'_e \vec{j}_e + w'_e \vec{k}_e = \eta_{e'} \vec{i}_{e'} - v'_{e'} \vec{j}_{e'} + w'_{e'} \vec{k}_{e'}, \quad (14)$$

where all functions are evaluated at the vertex  $\mathbf{v}$  and all derivatives are taken in direction  $\vec{i}_e$  or  $\vec{i}_{e'}$  correspondingly.

**Remark 3.2.** Let us comment on the information contained in the theorem. Equation (11) specifies the underlying inner product (in the terminology of Gelfand triples, it is the “pivot space”), while equation (12) prescribes the correct smoothness requirements on the individual fields (twice differentiable  $v, w$  and once differentiable  $u$  and  $\eta$ ). The form being semibounded<sup>5</sup> and closed tells us that it corresponds to a self-adjoint differential operator (“Hamiltonian”) which we will describe in the next theorem.

Perhaps the most practical consequence of this theorem is the set of matching conditions that are expressing the definition of joint rigidity in terms of the degrees of freedom of the beam — the displacement and angular displacement fields — written in the coordinate representation in which they enter the energy ( $v, w, u$  and  $\eta$ ). Given that  $\eta$  is the only coordinate of angular nature, it may mistakenly appear that continuity of rotation ought to be expressed as  $\eta_e = \eta_{e'}$ ; equation (14) is a reminder that  $\eta_e$  is just one component of rotation — the one around the axis of the beam — while the continuity must apply to the entire element of  $\text{SO}(3)$ .

To get to condition (14) we will parameterize small rotations in terms of the **rotation vector** we denote  $\omega$ .

**Lemma 3.3.** *The mapping  $\vec{\omega} \in \mathbb{R}^3 \mapsto \mathcal{R} \in \text{SO}(3)$  given by*

$$\mathcal{R} = \exp(\Omega), \quad (15)$$

where  $\Omega = \Omega(\vec{\omega})$  is a  $3 \times 3$  skew symmetric matrix acting as  $\vec{a} \mapsto \vec{\omega} \times \vec{a}$ , is a local  $C^\infty$ -diffeomorphism between a neighborhood of  $\vec{0}$  in  $\mathbb{R}^3$  and a neighborhood of  $\mathbb{I}$  in  $\text{SO}(3)$ . For small deformations of the beam characterized by  $\Psi = (v, w, u, \eta)$ , the corresponding  $\vec{\omega}(x)$  is

$$\vec{\omega}(x) = \eta(x) \vec{i} - v'(x) \vec{j} + w'(x) \vec{k} + \mathcal{O}(\|\Psi\|_{\mathfrak{h}(\Gamma)}^2), \quad (16)$$

where  $\{\vec{i}, \vec{j}, \vec{k}\}$  is the local basis of the beam and the norm is the Sobolev norm as in (12).

*Proof.* Exponential parameterization of  $\text{SO}(3)$  is standard; it is a local chart around  $\omega = \vec{0}$  which can be extended to cover all of  $\text{SO}(3)$  except rotations by  $\pi$  (around some axis). Expanding the exponential we get

$$\mathcal{R}\vec{a} = \vec{a} + \vec{\omega} \times \vec{a} + \mathcal{O}(|\vec{\omega}|^2), \quad (17)$$

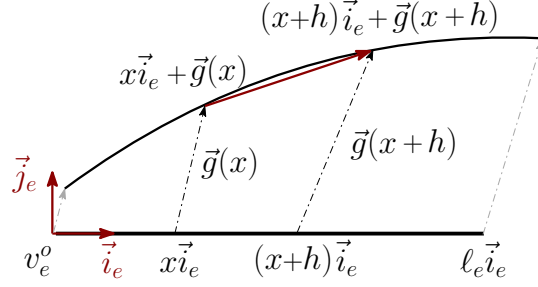
which are the leading terms in the so-called Euler–Rodrigues formula, more common in the applied literature (a discussion of this formula and its connection to exponential form (15) can be found in the Appendix). In particular, applying (17) to (1), we get

$$\vec{i}(x) = \vec{i} + \vec{\omega}(x) \times \vec{i} + \mathcal{O}(|\vec{\omega}|^2), \quad (18)$$

$$\vec{j}(x) = \vec{j} + \vec{\omega}(x) \times \vec{j} + \mathcal{O}(|\vec{\omega}|^2), \quad (19)$$

$$\vec{k}(x) = \vec{k} + \vec{\omega}(x) \times \vec{k} + \mathcal{O}(|\vec{\omega}|^2). \quad (20)$$

<sup>5</sup>In our case, it is semibounded below by 0, i.e. positive. Also note that semibounded implies (by definition) symmetric.

FIGURE 4. Displacement of points on beam  $e$ 

Substituting (19) into (5) we get

$$\eta(x) = \vec{\omega}(x) \cdot \vec{i} + \mathcal{O}(|\vec{\omega}|^2). \quad (21)$$

On the other hand, we can calculate  $\vec{i}(x)$  on an edge  $e$  from the corresponding  $\vec{g}(x)$ . The vector

$$\vec{\xi}(x) := \lim_{h \rightarrow 0} \frac{h\vec{i} + \vec{g}(x+h) - \vec{g}(x)}{h} = \vec{i} + \vec{g}'(x) \quad (22)$$

is a tangent vector to the beam  $e$  at point  $x$ . The extra term  $h\vec{i}$  appears because  $\vec{g}(x)$  is the displacement vector of the material point  $\mathbf{v}_e^o + x\vec{i}$ , not a position vector, see figure (4). To normalize  $\vec{\xi}(x)$ , observe the following relation for general vectors  $\vec{a}, \vec{b} \in \mathbb{R}^3$ ,

$$\frac{1}{|\vec{a} + \varepsilon\vec{b}|} = \frac{1}{|\vec{a}|} - \frac{\vec{a} \cdot \vec{b}}{|\vec{a}|^3} \varepsilon + \mathcal{O}(\varepsilon^2). \quad (23)$$

Applying this to (22) and using  $|\vec{i}| = 1$  we get

$$\vec{i}(x) := \frac{\vec{\xi}}{|\vec{\xi}|} = \vec{i} + \vec{g}'(x) - (\vec{i} \cdot \vec{g}'(x))\vec{i} + \mathcal{O}(|\vec{g}'|^2) \quad (24)$$

$$= \vec{i} + w'(x)\vec{j} + v'(x)\vec{k} + \mathcal{O}(|\vec{g}'|^2). \quad (25)$$

Comparing equation (25) with (18) and taking into account (21) we arrive to (16).

For future reference we also list here the expansions of other vectors in the deformed basis,

$$\vec{j}(x) = -w'(x)\vec{i} + \vec{j} + \eta(x)\vec{k} + \mathcal{O}(|\vec{g}'|^2), \quad \vec{k}(x) = -v'(x)\vec{i} - \eta(x)\vec{j} + \vec{k} + \mathcal{O}(|\vec{g}'|^2) \quad (26)$$

□

*Proof of Theorem 3.1.* We start by addressing the vertex matching condition. Equation (13) is simply the coordinate expansion (in the local coordinates of each edge) of the displacement continuity condition in Definition 1, equation (2a). Equation (14) is a direct application of Lemma 3.3 to condition (2b).

The form  $h$  defined by (10) is obviously positive and symmetric:

$$h[\Psi, \Psi] \geq 0 \quad \text{and} \quad h[\tilde{\Psi}, \Psi] = \overline{h[\Psi, \tilde{\Psi}]}. \quad (27)$$

To establish that  $h$  is closed, i.e. that the domain  $\text{Dom}(h)$  — the subspace of  $\tilde{\mathfrak{h}}(\Gamma)$  consisting of functions satisfying (13)-(14) — is complete with respect to the norm

$$\|\Psi\|_h := \|\Psi\|_{L^2(\Gamma)} + h[\Psi, \Psi], \quad (28)$$

we follow the standard procedure (see, for example, [5, Proof of Thm 1.4.11] or [17, Proof of Thm 4.3]). First we note that the space  $\tilde{\mathfrak{h}}(\Gamma)$  is complete with respect to its norm (the sum of Sobolev norms of individual spaces). Next, the operation of taking traces — vertex values of components of  $\Psi$  and their derivatives — is continuous in the Sobolev norm due to the standard inequalities (see [17, Lemma 4.2]),

$$|f(\mathbf{v}_e)|^2 \leq \frac{2}{|e|} \|f\|_{L^2(e)}^2 + |e| \|f'\|_{L^2(e)}^2, \quad \text{for any } f \in H^1(e), \quad (29)$$

$$|f'(\mathbf{v}_e)|^2 \leq \frac{2}{|e|} \|f'\|_{L^2(e)}^2 + |e| \|f''\|_{L^2(e)}^2, \quad \text{for any } f \in H^2(e), \quad (30)$$

where  $|e|$  is the length of the edge  $e$  and  $\mathbf{v}_e$  is one of its endpoints. Therefore  $\text{Dom}(h)$  is a closed subspace of  $\tilde{\mathfrak{h}}(\Gamma)$  and thus also complete with respect to the norm of  $\tilde{\mathfrak{h}}(\Gamma)$ . Finally, we observe that the  $h$ -norm (28) is equivalent to the Sobolev norm of  $\tilde{\mathfrak{h}}(\Gamma)$ , i.e.

$$c\|\Psi\|_{\tilde{\mathfrak{h}}(\Gamma)} \leq \|\Psi\|_{L^2(\Gamma)} + h[\Psi, \Psi] \leq C\|\Psi\|_{\tilde{\mathfrak{h}}(\Gamma)}, \quad (31)$$

for suitable constants  $c, C > 0$ . Here, for components  $v$  and  $w$  we use the inequality (see [8, Cor 4.2.7])

$$\|f'\|_{L^2(e)} \leq \alpha \left( \frac{1}{|e|} \|f\|_{L^2(e)} + |e| \|f''\|_{L^2(e)} \right), \quad (32)$$

for some  $\alpha > 0$  independent of  $f$ .  $\square$

**3.2. Joint conditions for the self-adjoint operator.** The main result of this paper characterizes the Hamiltonian of the frame as a self-adjoint differential operator on the metric graph.

**Theorem 3.4.** *Energy form (10) on a beam frame with free rigid joints corresponds to the self-adjoint operator  $H: L^2(\Gamma) \rightarrow L^2(\Gamma)$  acting as*

$$\Psi_e := \begin{pmatrix} v_e \\ w_e \\ u_e \\ \eta_e \end{pmatrix} \mapsto \begin{pmatrix} a_e v_e'''' \\ b_e w_e'''' \\ -c_e u_e'' \\ -d_e \eta_e'' \end{pmatrix} \quad (33)$$

on every edge  $e \in E$  of the graph. The domain of the operator  $H$  consists of the functions

$$\Psi \in \bigoplus_{e \in E} H^4(e) \oplus \bigoplus_{e \in E} H^4(e) \oplus \bigoplus_{e \in E} H^2(e) \oplus \bigoplus_{e \in E} H^2(e) =: \tilde{\mathfrak{H}}(\Gamma), \quad (34)$$

that satisfy, at each vertex  $\mathbf{v} \in V$ ,

(1) *continuity of displacement: for all  $e, e' \sim \mathbf{v}$ ,*

$$u_e \vec{i}_e + w_e \vec{j}_e + v_e \vec{k}_e = u_{e'} \vec{i}_{e'} + w_{e'} \vec{j}_{e'} + v_{e'} \vec{k}_{e'}, \quad (35)$$

(2) *continuity of rotation: for all  $e, e' \sim \mathbf{v}$ ,*

$$\eta_e \vec{i}_e - v_e' \vec{j}_e + w_e' \vec{k}_e = \eta_{e'} \vec{i}_{e'} - v_{e'}' \vec{j}_{e'} + w_{e'}' \vec{k}_{e'}, \quad (36)$$



(3) *balance of forces*

$$\sum_{e \sim \mathbf{v}} s_{\mathbf{v}}^e \left( c_e u_e' \vec{i}_e - b_e w_e''' \vec{j}_e - a_e v_e''' \vec{k}_e \right) = \vec{0}, \quad (37)$$

(4) *balance of moments*

$$\sum_{e \sim \mathbf{v}} s_{\mathbf{v}}^e \left( d_e \eta_e' \vec{i}_e - a_e v_e'' \vec{j}_e + b_e w_e'' \vec{k}_e \right) = \vec{0}. \quad (38)$$

Here  $n_{\mathbf{v}}$  is the degree of the vertex  $\mathbf{v}$ ,  $s_{\mathbf{v}}^e$  is the signed incidence indicator defined in section 2.3, all functions are evaluated at the vertex  $\mathbf{v}$ , and all derivatives on the edge  $e$  are taken in the direction  $\vec{i}_e$ .

**Remark 3.5.** Knowing that the operator is self-adjoint opens up many established mathematical tools for understanding the time evolution of the corresponding wave equation,

$$\frac{\partial^2 \Psi_e}{\partial t^2} = H \Psi_e, \quad e \in E.$$

For example, from the Spectral Theorem we immediately get orthogonality of the eigenfunctions (studied, in the engineering literature, in [11]). With little extra work (establishing compactness of the resolvent on frames which contain finitely many beams, each of finite length), one obtains existence of an eigenfunction basis.

**Remark 3.6.** Conditions (35) and (36), inherited from the domain of the sesquilinear form, encapsulate the rigid vertex assumption. Two additional conditions (37) and (38) are imposed to guarantee the operator is self-adjoint. These two conditions, derived from operator-theoretic considerations, have important physical meaning. Namely, they balance the forces and moments developed at the vertex as a result of relative displacement and angular displacement of edges adjacent to the vertex. In more details:

- (i) in condition (37),  $c_e u_e'$  is the force developed in direction  $\vec{i}_e$  due to in-axis tension of the edge  $e$ , while  $a_e v_e'''$  and  $b_e w_e'''$  are shear forces developed inside the edge in the directions  $\vec{k}_e$  and  $\vec{j}_e$ , respectively.
- (ii) in condition (38),  $d_e \eta_e'$  is the moment associated with angular displacement developed in direction  $\vec{i}_e$  due to in-axis rotation of the edge  $e$ , while  $a_e v_e''$  and  $b_e w_e''$  represent bending moments of the edge  $e$  in the directions  $\vec{j}_e$  and  $\vec{k}_e$ , respectively.

More details about the mechanics meaning of these quantities can be found in [52], in particular in sections 4.5 and 6.2 thereof.

**Remark 3.7.** It is instructive to see how the individual elements of conditions (35)–(38) change under the change of orientation of an edge  $e$ . Consider, for example, the change of local basis (omitting subscript  $e$  to avoid clutter)

$$\{\vec{i}, \vec{j}, \vec{k}\} \mapsto \{-\vec{i}, -\vec{j}, \vec{k}\}. \quad (39)$$

For convenience, we recall the definitions of the individual degrees of freedom,

$$v = \vec{k} \cdot \vec{g}, \quad w = \vec{j} \cdot \vec{g}, \quad u = \vec{i} \cdot \vec{g}, \quad \eta = \mathcal{R} \vec{j} \cdot \vec{k}, \quad (40)$$

where  $\vec{g}$  and  $\mathcal{R}$  are basis-independent quantities. In addition, all derivatives are taken in the direction  $\vec{i}$ , resulting in the sign change. We get

$$\begin{aligned} v &\mapsto v, & w &\mapsto -w, & u &\mapsto -u, & \eta &\mapsto -\eta, \\ v' &\mapsto -v', & w' &\mapsto w', & u' &\mapsto u', & \eta' &\mapsto \eta', \\ v'' &\mapsto v'', & w'' &\mapsto -w'', & & & & \\ v''' &\mapsto -v''', & w''' &\mapsto w''', & & & s_{\mathbf{v}}^e &\mapsto -s_{\mathbf{v}}^e. \end{aligned}$$

Combining with (39), we observe that all of the quantities

$$u\vec{i} + w\vec{j} + v\vec{k}, \quad \eta\vec{i} - v'\vec{j} + w'\vec{k}, \quad s_{\mathbf{v}}^e(cu'\vec{i} - bw'''\vec{j} - av'''\vec{k}), \quad \text{and} \quad s_{\mathbf{v}}^e(d\eta'\vec{i} - av''\vec{j} + bw''\vec{k})$$

remain invariant.

**Remark 3.8.** The formal proof of Theorem 3.4 given below is built around “knowing the right answer” and is not particularly instructive. In the present remark we *derive the right answer* while sacrificing some of the mathematical rigor.

We would like to represent the sesquilinear form as  $h[\tilde{\Psi}, \Psi] = \langle \tilde{\Psi}, H\Psi \rangle$ , so we integrate equation (10) by parts. This requires the field  $\Psi$  to be sufficiently smooth, an issue we ignore for now. We get

$$h[\tilde{\Psi}, \Psi] = \sum_{e \in E} \int_e (\tilde{v}_e v_e'''' + b_e \tilde{w}_e w_e'''' - c_e \tilde{u}_e u_e'' - d_e \tilde{\eta}_e \eta_e'') dx + \sum_{\mathbf{v} \in V} \mathcal{B}_{\mathbf{v}}, \quad (41)$$

where the boundary term  $\mathcal{B}_{\mathbf{v}}$  at vertex  $\mathbf{v}$  has the form

$$\mathcal{B}_{\mathbf{v}} := \sum_{e \sim \mathbf{v}} s_{\mathbf{v}}^e \left( a_e \tilde{v}'_e v''_e - a_e \tilde{v}_e v_e'''' + b_s \tilde{w}'_e w''_e - b_s \tilde{w}_e w_e'''' + c_e \tilde{u}_e u'_s + d_e \tilde{\eta}_e \eta'_e \right). \quad (42)$$

Since the field  $(\tilde{v}, \tilde{w}, \tilde{u}, \tilde{\eta})$  is arbitrary, the form of the differential operator  $H$  in  $\langle \tilde{\Psi}, H\Psi \rangle$  is clear, as long as the boundary terms disappear:  $\mathcal{B}_{\mathbf{v}} = 0$  for all  $\mathbf{v}$ .

Applying the fact that  $\{\vec{i}_e, \vec{j}_e, \vec{k}_e\}$  is an orthonormal basis, for each  $e \sim \mathbf{v}$  we can write

$$c_e \tilde{u}_e u'_e - b_e \tilde{w}_e w_e'''' - a_e \tilde{v}_e v_e'''' \tilde{v}_e = \underbrace{(\tilde{u}_e \vec{i}_e + \tilde{w}_e \vec{j}_e + \tilde{v}_e \vec{k}_e)}_{=\vec{g}_e(\mathbf{v})} \cdot (c_e u'_e \vec{i}_e - b_e w_e'''' \vec{j}_e - a_e v_e'''' \vec{k}_e) \quad (43)$$

and similarly

$$d_e \tilde{\eta}_e \eta'_e + b_e \tilde{w}'_e w''_e + a_e \tilde{v}'_e v''_e = \underbrace{(\tilde{\eta}_e \vec{i}_e - \tilde{v}'_e \vec{j}_e + \tilde{w}'_e \vec{k}_e)}_{=\vec{\omega}_e(\mathbf{v})} \cdot (d_e \eta'_e \vec{i}_e - a_e v_e'' \vec{j}_e + b_e w_e'' \vec{k}_e) \quad (44)$$

Summing over  $e \sim \mathbf{v}$  along with the fact that the displacement  $\vec{g}_e(\mathbf{v})$  and rotation vector  $\vec{\omega}_e(\mathbf{v})$  are independent of  $e \sim \mathbf{v}$ , we arrive to the condition

$$\mathcal{B}_{\mathbf{v}} = \vec{g}_e(\mathbf{v}) \cdot \sum_{e \sim \mathbf{v}} s_{\mathbf{v}}^e (c_e u'_e \vec{i}_e - b_e w_e'''' \vec{j}_e - a_e v_e'''' \vec{k}_e) + \vec{\omega}_e(\mathbf{v}) \cdot \sum_{e \sim \mathbf{v}} s_{\mathbf{v}}^e (d_e \eta'_e \vec{i}_e - a_e v_e'' \vec{j}_e + b_e w_e'' \vec{k}_e) = 0 \quad (45)$$

Since the vectors  $\vec{g}_e(\mathbf{v})$  and  $\vec{\omega}_e(\mathbf{v})$  are arbitrary,  $\mathcal{B}_{\mathbf{v}} = 0$  only if the two sums in front of  $\vec{g}_e(\mathbf{v})$  and  $\vec{\omega}_e(\mathbf{v})$  vanish. This results in conditions (37) and (38) correspondingly.

We now proceed to the formal proof of Theorem 3.4.

*Proof of Theorem 3.4.* By the Representation Theorem of sesquilinear forms (see [22, section VI.2] or [46, Thm. 10.7 and Cor. 10.8]), the form  $h$  of Theorem 3.1 corresponds to a self-adjoint operator  $H$  such that  $\text{Dom}(H) \subset \text{Dom}(h)$  and

$$h[\tilde{\Psi}, \Psi] = \langle \tilde{\Psi}, H\Psi \rangle \quad \text{for all } \tilde{\Psi} \in \text{Dom}(h), \Psi \in \text{Dom}(H). \quad (46)$$

Moreover, the self-adjoint operator satisfying this condition is unique.

Since  $\Psi \in \text{Dom}(H) \subset \tilde{\mathfrak{H}}(\Gamma)$ , the integration by parts performed in (41) is valid and equation (45) shows that condition (46) is satisfied. Therefore we only need to establish that the operator  $H$  defined in the Theorem is indeed self-adjoint, i.e.  $H^* = H$ .

The first step is to obtain a ‘‘bound’’ on the domain of  $H^*$ : prove that  $\text{Dom}(H^*) \subset \tilde{\mathfrak{H}}(\Gamma)$  which guarantees enough smoothness of  $\tilde{\Psi} \in \text{Dom}(H^*)$  to integrate by parts freely. The standard trick is as follows: consider the operator  $H_{\min}$  which is given by the differential expression (33) with the domain consisting of functions from  $\tilde{\mathfrak{H}}(\Gamma)$  with additional conditions<sup>6</sup> at every vertex  $\mathbf{v}$

$$v_e = v'_e = v''_e = v'''_e = 0, \quad w_e = w'_e = w''_e = w'''_e = 0, \quad u_e = u'_e = 0, \quad \eta_e = \eta'_e = 0. \quad (47)$$

The operator  $H_{\min}$  decomposes into a direct sum of operators each acting on a single edge  $e$  and a single component  $u, v, w$  or  $\eta$ . The standard calculation (see [46, Example 1.4]) shows that the adjoint  $H_{\min}^*$  is given by the same differential expression (33) with the domain equal to *all* of  $\tilde{\mathfrak{H}}(\Gamma)$ . Now we obviously have  $H_{\min} \subset H \subset H_{\min}^*$  (all operators act the same and the inclusion should be understood as inclusion of domains), therefore  $H_{\min} \subset H^* \subset H_{\min}^*$ , in particular  $\text{Dom}(H^*) \subset \tilde{\mathfrak{H}}(\Gamma)$  and  $H^*$  also acts as (33).

The second step is to observe that for *any* operators  $S_1$  and  $S_2$  satisfying  $H_{\min} \subseteq S_i \subseteq H_{\min}^*$ ,  $i = 1, 2$ , we can integrate by parts to get

$$\langle \tilde{\Psi}, S_1\Psi \rangle - \langle S_2\tilde{\Psi}, \Psi \rangle = \Omega[\tilde{\Psi}, \Psi], \quad (48)$$

where

$$\Omega[\tilde{\Psi}, \Psi] = \sum_{\mathbf{v}, e \sim \mathbf{v}} \vec{g}_e \cdot (c_e \tilde{u}'_e \vec{i}_e - b_e \tilde{w}'''_e \vec{j}_e - a_e \tilde{v}'''_e \vec{k}_e) s_{\mathbf{v}}^e + \vec{\omega}_e \cdot (d_e \tilde{\eta}'_e \vec{i}_e - a_e \tilde{v}''_e \vec{j}_e + b_e \tilde{w}''_e \vec{k}_e) s_{\mathbf{v}}^e \quad (49)$$

$$- \vec{g}_e \cdot (c_e u'_e \vec{i}_e - b_e w'''_e \vec{j}_e - a_e v'''_e \vec{k}_e) s_{\mathbf{v}}^e - \vec{\omega}_e \cdot (d_e \eta'_e \vec{i}_e - a_e v''_e \vec{j}_e + b_e w''_e \vec{k}_e) s_{\mathbf{v}}^e, \quad (50)$$

with all functions evaluated at  $\mathbf{v}$ . This is known as the ‘‘Green’s identity’’.

The third step is to show that  $H$  is symmetric, i.e.

$$\langle \tilde{\Psi}, H\Psi \rangle - \langle H\tilde{\Psi}, \Psi \rangle = 0 \quad \text{for all } \Psi, \tilde{\Psi} \in \text{Dom}(H). \quad (51)$$

We use (48) with  $S_1 = S_2 = H$  and note that both  $\Psi$  and  $\tilde{\Psi}$  satisfy conditions (35)–(38), yielding  $\Omega[\tilde{\Psi}, \Psi] = 0$  as required. This establishes that our conditions are restrictive enough:  $\text{Dom}(H) \subset \text{Dom}(H^*)$ .

Finally, we show that the conditions are not excessively restrictive, i.e.  $\text{Dom}(H^*) \subset \text{Dom}(H)$ . We start with a  $\tilde{\Psi} \in \text{Dom}(H^*)$  which means that

$$\langle \tilde{\Psi}, H\Psi \rangle - \langle H^*\tilde{\Psi}, \Psi \rangle = 0 \quad \text{for all } \Psi \in \text{Dom}(H). \quad (52)$$

Using (48) again, now with  $S_1 = H$  and  $S_2 = H^*$ , we get  $\Omega[\tilde{\Psi}, \Psi] = 0$ . Using that  $\Psi$  is arbitrary within  $\text{Dom}(H)$ , a bit of linear algebra proves that  $\tilde{\Psi}$  must also satisfy (35)–(38).  $\square$

<sup>6</sup>These conditions are too restrictive for self-adjointness.

## 4. SOME EXTENSIONS AND SPECIAL CASES

**4.1. Dummy vertices.** As an important check on the consistency of the conditions we derived we show that any point in the interior of a beam can be considered a free rigid joint of two co-linear beams (and vice versa).

**Lemma 4.1.** *Let  $\mathbf{v}$  be a free rigid joint of degree 2 and the beams incident to it have identical material properties and be co-linear, i.e.  $\{\vec{i}_1, \vec{j}_1, \vec{k}_1\} = \{\vec{i}_2, \vec{j}_2, \vec{k}_2\}$  up to a sign change of an even number of vectors. Then  $\Psi_{e_1}$  and  $\Psi_{e_2}$  agree at  $\mathbf{v}$  including derivatives (of order 1 for  $u$  and  $\eta$  and order 3 for  $v$  and  $w$ ) and therefore the union of  $e_1$  and  $e_2$  may be represented as a single edge  $e$  with  $\Psi_e \in \tilde{\mathfrak{H}}(\Gamma)$ .*

*Proof.* Assume, for now, that  $\{\vec{i}_1, \vec{j}_1, \vec{k}_1\} = \{\vec{i}_2, \vec{j}_2, \vec{k}_2\}$ . This means that the end  $e_1$  meets the origin of  $e_2$  (or vice versa) and therefore  $s_{\mathbf{v}}^{e_1} = -s_{\mathbf{v}}^{e_2}$ . Evaluating components of conditions (35)–(38) with respect to the common basis  $\{\vec{i}_1, \vec{j}_1, \vec{k}_1\}$ , we get for the values of the corresponding functions at  $\mathbf{v}$

$$u_{e_1} = u_{e_2}, \quad u'_{e_1} - u'_{e_2} = 0, \quad v_{e_1} = v_{e_2}, \quad v'_{e_1} = v'_{e_2}, \quad v''_{e_1} - v''_{e_2} = 0, \quad v'''_{e_1} - v'''_{e_2} = 0, \quad (53)$$

and so on. To understand other cases of bases arrangements, for example, the case  $\{\vec{i}_1, \vec{j}_1, \vec{k}_1\} = \{-\vec{i}_2, -\vec{j}_2, \vec{k}_2\}$ , we refer to Remark 3.7.  $\square$

**4.2. Planar frame.** A particularly well-studied case in the literature is the planar frame, which in its un-deformed configuration is embedded in a two dimensional plane. Without loss of generality assume that this plane has normal vector  $\vec{E}_3$ . We also assume that for all edges  $e$ ,  $\vec{k}_e$  is chosen to be the same,  $\vec{k}_e = \vec{k} = \vec{E}_3$  (in particular this requires that the principal axes of inertia of every beam can be aligned accordingly).

In this situation the Hamiltonian of the frame decouples into two operators, one linking out-of-plane displacement with angular displacement (cf. Chapter 1 in [35]) and the other linking in-plane displacement with axial displacement.

**Corollary 4.2.** *Free planar network of beams with free rigid joints is described by Hamiltonian  $H = H_1 \oplus H_2$  where  $H_1$  is a differential operator acting as*

$$\Psi_{e,1} := \begin{pmatrix} v_e \\ \eta_e \end{pmatrix} \mapsto \begin{pmatrix} a_e v_e''' \\ -d_e \eta_e'' \end{pmatrix} \quad (54)$$

on functions  $\Psi_{e,1} \in \bigoplus_{e \in E} H^4(e) \oplus \bigoplus_{e \in E} H^2(e)$  satisfying at each vertex  $\mathbf{v}$  the primary (form domain) conditions

$$v_e = v_{e'}, \quad \forall e, e' \sim \mathbf{v}, \quad (55a)$$

$$\eta_1 \vec{i}_1 - v'_1 \vec{j}_1 = \eta_{e'} \vec{i}_{e'} - v'_{e'} \vec{j}_{e'}, \quad \forall e, e' \sim \mathbf{v}, \quad (55b)$$

and the secondary conditions

$$\sum_{e \sim \mathbf{v}} s_{\mathbf{v}}^e a_e v_e''' = 0, \quad (56a)$$

$$\sum_{e \sim \mathbf{v}} s_{\mathbf{v}}^e (d_e \eta_e' \vec{i}_e - a_e v_e'' \vec{j}_e) = \vec{0}. \quad (56b)$$

The operator  $H_2$  acts as

$$\Psi_{e,2} := \begin{pmatrix} w_e \\ u_e \end{pmatrix} \mapsto \begin{pmatrix} b_e w_e'''' \\ -c_e u_e'' \end{pmatrix} \quad (57)$$

on functions  $\Psi_{e,2} \in \bigoplus_{e \in E} H^4(e) \oplus \bigoplus_{e \in E} H^2(e)$  satisfying at each vertex  $\mathbf{v}$  the primary (form domain) conditions

$$u_e \vec{i}_e + w_e \vec{j}_e = u_{e'} \vec{i}_{e'} + w_{e'} \vec{j}_{e'}, \quad \forall e, e' \sim \mathbf{v}, \quad (58a)$$

$$w'_e = w'_{e'}, \quad \forall e, e' \sim \mathbf{v}, \quad (58b)$$

and secondary conditions

$$\sum_{e \sim \mathbf{v}} s_{\mathbf{v}}^e (c_e u'_e \vec{i}_e - b_e w_e'' \vec{j}_e) = \vec{0}, \quad (59a)$$

$$\sum_{e \sim \mathbf{v}} s_{\mathbf{v}}^e b_e w_e'' = \vec{0}. \quad (59b)$$

*Proof.* The differential expression for the operator  $H$  is already in the “block-diagonal” form, see (33), so it remains to show that the vertex conditions decompose as described. But that follows directly from projecting conditions (35)–(38) onto the common normal  $\vec{k}$  and onto its orthogonal complement.  $\square$

One of the vertex conditions used in mathematical literature dealing with planar beam networks is that the beams remain locally planar when deformed, see e.g. [7] and [23]. This property is now a part of vertex condition (55b) as shown in the next Lemma. In fact, condition (55b) contains more information due to the fact that we now have an extra degree of freedom (angular displacement  $\eta(x)$ ) in comparison to [7, 23]. We also note that condition (55b) does not require special consideration for certain values of angles between beams, cf. [23, Theorem 1].

**Lemma 4.3.** *Condition (55b) holds if and only if for any  $e \sim \mathbf{v}$*

$$(\vec{j}_2 \cdot \vec{i}_e) v'_1 + (\vec{j}_e \cdot \vec{i}_1) v'_2 + (\vec{j}_1 \cdot \vec{i}_2) v'_e = 0, \quad (60)$$

$$(\vec{j}_2 \cdot \vec{j}_e) v'_1 - (\vec{j}_e \cdot \vec{j}_1) v'_2 + (\vec{j}_1 \cdot \vec{i}_2) \eta_e = 0. \quad (61)$$

Equation (60) is equivalent to the requirement that all vectors  $\{\vec{i}_e(\mathbf{v})\}_{e \sim \mathbf{v}}$  lie in the same plane.

The proof of the lemma is technical and is deferred to Appendix B.

**Remark 4.4.** In the special case of degree  $n = 2$ , condition (60) becomes vacuous, reducing to  $v'_1 = v'_1$  and  $v'_2 = v'_2$ .

**4.3. Self-adjoint extension including vertex energy.** Here we describe a range of vertex conditions achieved by introducing vertex energy in (10). Consider the energy form

$$\mathcal{U}^{(\Gamma)} = \sum_{e \in E} \mathcal{U}^{(e)} + \sum_{\mathbf{v} \in V} \mathcal{U}^{(\mathbf{v})} \quad (62)$$

with vertex energy defined as

$$\mathcal{U}^{(\mathbf{v})} := \frac{1}{2} (|\vec{g}_{\mathbf{v}}|^2 \tan(\alpha_{\mathbf{v}}) + |\vec{\omega}_{\mathbf{v}}|^2 \tan(\beta_{\mathbf{v}})) \quad (63)$$

In (63) the parameters  $\alpha_{\mathbf{v}}, \beta_{\mathbf{v}} \in (-\pi/2, \pi/2)$  and  $\vec{g}_{\mathbf{v}} := \vec{g}_e(\mathbf{v})$  and  $\vec{\omega}_{\mathbf{v}} := \vec{\omega}_e(\mathbf{v})$  for any  $e$  adjacent to  $\mathbf{v}$ . We then arrive to the following modification of Theorem 3.4.

**Theorem 4.5.** *Free network of beams with energy functional (62) along with rigid vertex condition is described by the Hamiltonian  $H$  acting as (33) that satisfies at each vertex  $\mathbf{v} \in V$  of degree  $n_{\mathbf{v}}$ ,*

(i) *continuity of displacement: for all  $e, e' \sim \mathbf{v}$ ,*

$$u_e \vec{i}_e + w_e \vec{j}_e + v_e \vec{k}_e = u_{e'} \vec{i}_{e'} + w_{e'} \vec{j}_{e'} + v_{e'} \vec{k}_{e'} =: \vec{g}_{\mathbf{v}} \quad (64)$$

(ii) *continuity of rotation: for all  $e, e' \sim \mathbf{v}$ ,*

$$\eta_e \vec{i}_e - v'_e \vec{j}_e + w'_e \vec{k}_e = \eta_{e'} \vec{i}_{e'} - v'_{e'} \vec{j}_{e'} + w'_{e'} \vec{k}_{e'} =: \vec{\omega}_{\mathbf{v}} \quad (65)$$

(iii) *balance of forces*

$$\vec{g}_{\mathbf{v}} \sin(\alpha_{\mathbf{v}}) + \cos(\alpha_{\mathbf{v}}) \sum_{e \sim \mathbf{v}} s_{\mathbf{v}}^e (c_e u'_e \vec{i}_e - b_e w''_e \vec{j}_e - a_e v'''_e \vec{k}_e) = 0, \quad (66)$$

(iv) *balance of moments*

$$\vec{\omega}_{\mathbf{v}} \sin(\beta_{\mathbf{v}}) + \cos(\beta_{\mathbf{v}}) \sum_{e \sim \mathbf{v}} s_{\mathbf{v}}^e (d_e \eta'_e \vec{i}_e - a_e v''_e \vec{j}_e + b_e w''_e \vec{k}_e) = 0. \quad (67)$$

We omit the proof of this Theorem as it is analogous to the proof of Theorem 3.4.

Setting  $\alpha_{\mathbf{v}} = \beta_{\mathbf{v}} = 0$  in the above Theorem we recover the free rigid joint conditions of Theorem 3.4. While the value  $\pi/2$  is excluded from the allowed range of  $\alpha_{\mathbf{v}}$  and  $\beta_{\mathbf{v}}$  in the energy form (63), the corresponding Hamiltonian remains self-adjoint, with conditions becoming

$$u_e \vec{i}_e + w_e \vec{j}_e + v_e \vec{k}_e = 0 \quad (68)$$

or

$$\eta_e \vec{i}_e - v'_e \vec{j}_e + w'_e \vec{k}_e = 0 \quad (69)$$

with  $\alpha_{\mathbf{v}} = \pi/2$  or  $\beta_{\mathbf{v}} = \pi/2$  correspondingly. As usual with Dirichlet-type conditions, they have to be introduced into the domain of the form directly, hence the divergence of (63).

The choices  $\{\alpha_{\mathbf{v}}, \beta_{\mathbf{v}}\} \in \{0, \pi/2\}$  cover several physically relevant conditions. For a vertex of degree  $n = 1$  we summarize these conditions in Table 1, listing the names commonly used in applied literature. Note that many more variations of the conditions can be formulated (and are of great practical relevance), where the displacement or rotation are not completely free or completely zero, but are restricted to certain subspaces.

**Remark 4.6.** It is also possible to classify *all* conditions leading to a self-adjoint operator (33), using, for example, symplectic linear algebra [6, Theorem 3.1] or other methods [5, Theorem 1.4.1].

## 5. SPECTRAL ANALYSIS BY EXAMPLE

**5.1. General strategy.** Calculating eigenvalues of the operator  $H$  described in Theorem 3.4 is the main step towards understanding of vibration of beam frames. The most direct approach is to solve the eigenvalue equation  $H\Psi = \lambda\Psi$  component-wise on every edge before applying conditions at vertices. For example, the equation on the out-of-plane displacement  $v_e$  on an edge  $e$  reads

$$a_e \frac{d^4 v_e(x)}{dx^4} = \lambda v_e(x), \quad (70)$$

with the general solution (assuming  $\lambda \neq 0$ ),

$$v_e(x) = C_{e,1}^v \cosh(\mu_e x) + C_{e,2}^v \sinh(\mu_e x) + C_{e,3}^v \cos(\mu_e x) + C_{e,4}^v \sin(\mu_e x), \quad \mu_e := (\lambda/a_e)^{1/4}. \quad (71)$$

Type	$\alpha_{\mathbf{v}}$	$\beta_{\mathbf{v}}$	Boundary Types	
			Primary	Secondary
Free	0	0	—	$u'_{\mathbf{v}} = w'''_{\mathbf{v}} = v'''_{\mathbf{v}} = 0$ $\eta'_{\mathbf{v}} = v''_{\mathbf{v}} = w''_{\mathbf{v}} = 0$
Fixed (Clamped)	$\pi/2$	$\pi/2$	$u_{\mathbf{v}} = w_{\mathbf{v}} = v_{\mathbf{v}} = 0$ $\eta_{\mathbf{v}} = v'_{\mathbf{v}} = w'_{\mathbf{v}} = 0$	—
Pinned	$\pi/2$	0	$u_{\mathbf{v}} = w_{\mathbf{v}} = v_{\mathbf{v}} = 0$	$\eta'_{\mathbf{v}} = v''_{\mathbf{v}} = w''_{\mathbf{v}} = 0$
Guided	0	$\pi/2$	$\eta_{\mathbf{v}} = v'_{\mathbf{v}} = w'_{\mathbf{v}} = 0$	$u'_{\mathbf{v}} = w'''_{\mathbf{v}} = v'''_{\mathbf{v}} = 0$

TABLE 1. Some boundary conditions for a vertex of degree one.

The eigenvalue equation for the in-axis angular displacement is

$$-d_e \frac{d^2 \eta_e(x)}{dx^2} = \lambda \eta_e(x), \quad (72)$$

with the general solution

$$\eta_e(x) = C_{e,1}^{\eta} \cos(\beta_e x) + C_{e,2}^{\eta} \sin(\beta_e x), \quad \beta_e := (\lambda/d_e)^{1/2}, \quad (73)$$

and so on. Vertex conditions (35)–(38) imposed at the ends of the edges couple together different solutions and lead to a homogeneous linear system on the constants  $\{C_{e,j}^*\}$ . The coefficients of this linear system are trigonometric functions of  $\lambda$  and edge lengths. Eigenvalues  $\lambda$  are characterized by the existence of a non-trivial choice of the constants  $\{C_{e,j}^*\}$ , which can be detected by equating the system's determinant to zero. This condition is known as the dynamic stiffness method in engineering literature [3] and is analogous to “characteristic” or “secular” equation used in the study of quantum graphs [49, 24].

However, problems can quickly become computationally overwhelming since there are 12 constants  $C_{e,j}^*$  associated with every beam. In section 5.3 we simplify an example using symmetry, which is frequently present in real-life applications. This technique, based on representation theory of finite groups, allows one to decompose the original problem into a sum of operators each corresponding to a particular class of vibrational modes.

We note that a particular example of such decomposition is the decoupling of Corollary 4.2 for a planar frame. Indeed, all planar graphs enjoy the symmetry of reflection across the  $X - Y$  (or  $E_1 - E_2$ ) plane. The operator  $H_1$  of Corollary 4.2 encapsulates the part of the operator  $H$  which is anti-symmetric with respect to this reflection.

**5.2. Example: a simple planar graph.** Consider the *planar* beam frame depicted in Figure 5 consisting of three beams  $e_1, e_2, e_3$  meeting at the free rigid joint  $\mathbf{v}_c$ . The endpoints  $\mathbf{v}_1, \mathbf{v}_2$  and  $\mathbf{v}_3$  are assumed to be fixed, see Table 1. The beams are oriented from the fixed ends to the joint; the local basis of each beam is shown in the Figure.

We focus our attention on the out-of-plane displacement of the beam frame, which, according to Corollary 4.2, is coupled to the angular displacement. The eigenvalue problem for the operator  $H_1$  satisfies equations (70) and (72) on each edge. Imposing the conditions at the boundary vertices

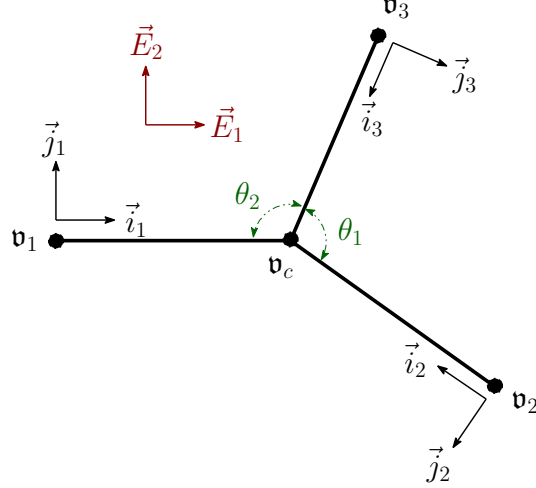


FIGURE 5. Geometry of planar star graph in its equilibrium state.

$\mathbf{v}_1, \mathbf{v}_2, \mathbf{v}_3$ , the general solutions reduce to

$$v_i(x) = A_i(\sinh(\mu_i x) - \sin(\mu_i x)) + B_i(\cosh(\mu_i x) - \cos(\mu_i x)), \quad \eta_i(x) = C_i \sin(\beta_i x), \quad (74)$$

with  $\mu_i := (\lambda/a_i)^{1/4}$  and  $\beta_i = (\lambda/d_i)^{1/2}$ . Applying vertex conditions (55) and (56) to (74), the eigenvalue problem reduces to finding the coefficient vector  $(A_1 \ B_1 \ A_2 \ B_2 \ A_3 \ B_3 \ C_1 \ C_2 \ C_3)^T$  in the kernel of the  $9 \times 9$  matrix  $M = M(\lambda)$  given by

$$M = \begin{pmatrix} S_{\mu_1 \ell_1}^- & C_{\mu_1 \ell_1}^- & 0 & -S_{\mu_2 \ell_2}^- & -C_{\mu_2 \ell_2}^- & 0 & 0 & 0 & 0 \\ S_{\mu_1 \ell_1}^- & C_{\mu_1 \ell_1}^- & 0 & 0 & 0 & 0 & -S_{\mu_3 \ell_3}^- & -C_{\mu_3 \ell_3}^- & 0 \\ \mu_1 C_{\mu_1 \ell_1}^+ & \mu_1 S_{\mu_1 \ell_1}^- & 0 & \mu_2 C_{\mu_2 \ell_2}^+ & \mu_2 S_{\mu_2 \ell_2}^- & 0 & \mu_3 C_{\mu_3 \ell_3}^+ & \mu_3 S_{\mu_3 \ell_3}^- & 0 \\ 0 & 0 & S_{\beta_1 \ell_1} & S_{\alpha_1 \mu_2} C_{\mu_2 \ell_2}^- & S_{\alpha_1 \mu_2} S_{\mu_2 \ell_2}^+ & -C_{\alpha_1} S_{\beta_2 \ell_2} & 0 & 0 & 0 \\ 0 & 0 & S_{\beta_1 \ell_1} & 0 & 0 & 0 & -S_{\alpha_2} \mu_3 C_{\mu_3 \ell_3}^- & -S_{\alpha_2} \mu_3 S_{\mu_3 \ell_3}^+ & -C_{\alpha_2} S_{\beta_3 \ell_3} \\ -\mu_1 C_{\mu_1 \ell_1}^- & -\mu_1 S_{\mu_1 \ell_1}^+ & 0 & C_{\alpha_1} \mu_2 C_{\mu_2 \ell_2}^- & C_{\alpha_1} \mu_2 S_{\mu_2 \ell_2}^+ & S_{\alpha_1} S_{\beta_2 \ell_2} & 0 & 0 & 0 \\ -\mu_1 C_{\mu_1 \ell_1}^- & -\mu_1 S_{\mu_1 \ell_1}^+ & 0 & 0 & 0 & 0 & C_{\alpha_2} \mu_3 C_{\mu_3 \ell_3}^- & C_{\alpha_2} \mu_3 S_{\mu_3 \ell_3}^+ & -S_{\alpha_2} S_{\beta_3 \ell_3} \\ \mu_1^2 S_{\mu_1 \ell_1}^+ & \mu_1^2 C_{\mu_1 \ell_1}^+ & 0 & C_{\alpha_1} \mu_2^2 S_{\mu_2 \ell_2}^+ & C_{\alpha_1} \mu_2^2 C_{\mu_2 \ell_2}^- & S_{\alpha_1} \beta_2 C_{\beta_2 \ell_2} & C_{\alpha_2} \mu_3^2 S_{\mu_3 \ell_3}^+ & C_{\alpha_2} \mu_3^2 C_{\mu_3 \ell_3}^- & -S_{\alpha_2} \beta_3 S_{\beta_3 \ell_3} \\ 0 & 0 & \beta_1 C_{\beta_1 \ell_1} & S_{\alpha_1} \mu_2^2 S_{\mu_2 \ell_2}^+ & -S_{\alpha_1} \mu_2^2 C_{\mu_2 \ell_2}^- & C_{\alpha_1} \beta_2 C_{\beta_2 \ell_2} & S_{\alpha_2} \mu_3^2 S_{\mu_3 \ell_3}^+ & S_{\alpha_2} \mu_3^2 C_{\mu_3 \ell_3}^- & C_{\alpha_2} \beta_3 C_{\beta_3 \ell_3} \end{pmatrix}$$

with the corresponding eigenvalue  $\lambda$  being a solution of  $\det(M_\lambda) = 0$ . We used the following abbreviations to make the matrix more compact

$$S_\gamma := \sin(\gamma), \quad C_\gamma := \cos(\gamma), \quad S_\gamma^\pm := \sinh(\gamma) \pm \sin(\gamma), \quad C_\gamma^\pm := \cosh(\gamma) \pm \cos(\gamma), \quad (75)$$

Results of numerical calculation are shown in Figures 6 and 7 for  $\theta_1 = \pi$  and  $\theta_2 = \pi/2$  (see Figure 5). Figure 6 shows displacement of the first two eigenfunctions where all beams' properties are selected identically. Unit value is selected for all the parameters and the length of beams, i.e. for all beams we set  $a_i = 1$  and  $d_i = 1$  (these parameters appear in definition of  $\mu_i$ 's and  $\beta_i$ 's above). The color represents the in-axis angular displacement of the beams.

Increasing the edge's resistance to angular displacement strongly affects the form of the eigenfunction. In the limiting case where  $d_i \rightarrow \infty$ , the tangent plane at vertex  $c$  does not change its angle (remains horizontal). Figure 7 shows the plots of displacement eigenfunction along with the value of angular displacement for  $a_i = 1$  and  $d_i = 10^3$  for  $i = 1, 2, 3$ .

**5.3. Example of a three dimensional graph: antenna tower.** Next we apply conditions of Theorem 3.4 to study eigenmodes of a three dimensional star graph. Our particular choice is a graph with a high degree of symmetry, which is frequent in applications. This will allow us



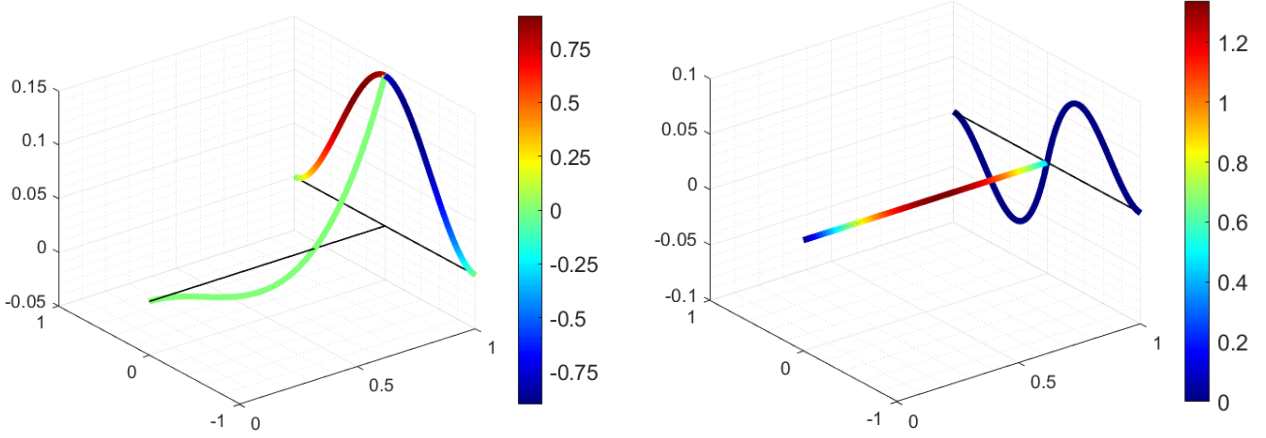


FIGURE 6. Eigenfuctions corresponding to first and second eigenvalues for parameters  $a_1 = a_2 = a_3 = 1$  and  $d_1 = d_2 = d_3 = 1$ . Color bar shows value of in-axis angular displacement of edges.

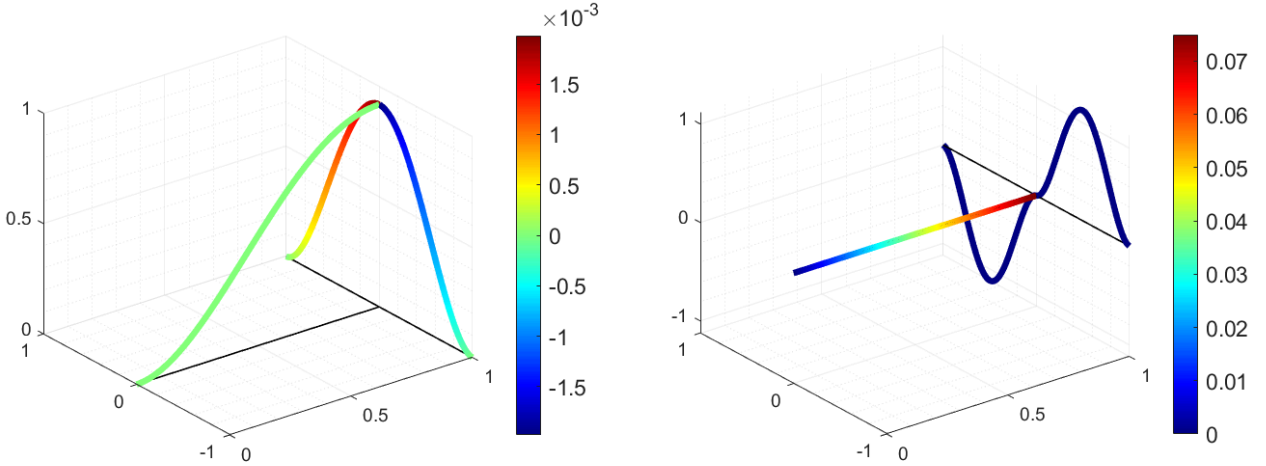


FIGURE 7. Eigenfuctions corresponding to first and second eigenvalues for parameters  $a_1 = a_2 = a_3 = 1$  and  $d_1 = d_2 = d_3 = 10^3$ . Color bar shows value of in-axis angular displacement of edges.

to demonstrate the use of group representation theory to classify eigenmodes and simplify their analysis. Let  $\Gamma_{AT}$  be the graph formed by three leg beams  $e_1, e_2, e_3$  and a vertical “antenna” beam  $e_0$ , all joining at the internal vertex  $\mathbf{v}_c$ , see Figure 8. The structure and its material parameters are assumed to be symmetric with respect to rotation by  $2\pi/3$  around the vertical axis and with respect to reflection swapping a pair of the leg beams. This implies that  $a_0 = b_0$  and that the leg beams are identical with principal axes of inertia that may be chosen to have  $\vec{j}_n \perp \vec{E}_3$  for  $n = 1, 2, 3$ , see Figure 8 and equation (81) below. The leg ends  $\mathbf{v}_1, \mathbf{v}_2, \mathbf{v}_3$  are clamped (vanishing displacement and angular displacement), vertex  $\mathbf{v}_c$  is a free rigid joint and the end  $\mathbf{v}_0$  of the vertical beam is free.

Our main result of the section is a decomposition of the operator  $H$  into a direct sum of four self-adjoint operators. We will later analyse each part separately.

**Theorem 5.1.** *The Hamiltonian operator  $H$  of the beam frame  $\Gamma_{AT}$  is reduced by the decomposition*

$$L^2(\Gamma) = \mathcal{H}_{\text{trv}} \oplus \mathcal{H}_{\text{alt}} \oplus \mathcal{H}_\omega \oplus \overline{\mathcal{H}_\omega}, \quad (76)$$

where

$$\mathcal{H}_{\text{trv}} := \{ \Psi \in L^2(\Gamma) : v_0 = w_0 = \eta_0 = 0, w_s = \eta_s = 0, v_1 = v_2 = v_3, u_1 = u_2 = u_3 \}, \quad (77)$$

$$\mathcal{H}_{\text{alt}} := \{ \Psi \in L^2(\Gamma) : v_0 = w_0 = u_0 = 0, u_s = v_s = 0, w_1 = w_2 = w_3, \eta_1 = \eta_2 = \eta_3 \}, \quad (78)$$

$$\mathcal{H}_\omega := \{ \Psi \in L^2(\Gamma) : u_0 = \eta_0 = 0, w_0 = i v_0, \Psi_3 = \omega \Psi_2 = \omega^2 \Psi_1 \} = \overline{\mathcal{H}_\omega}, \quad (79)$$

where  $s \in \{1, 2, 3\}$  labels the legs,  $\Psi_s := (v_s, w_s, u_s, \eta_s)^T$ , and  $\omega = e^{2\pi i/3}$ .

**Remark 5.2.** A decomposition  $\mathcal{H} = \bigoplus_\rho \mathcal{H}_\rho$  is **reducing** for an operator  $H$  if  $H$  is invariant on each of the subspaces and the operator domain  $\text{Dom}(H)$  is ‘‘aligned’’ with respect to the decomposition, namely

$$\text{Dom}(H) = \bigoplus_\rho (\mathcal{H}_\rho \cap \text{Dom}(H)).$$

More precisely, the operator  $H$  is required to commute with the orthogonal projector  $\mathbf{P}_\rho$  onto  $\mathcal{H}_\rho$ . This means that we can restrict  $H$  to each subspace in turn and every aspect of the spectral data of the operator  $H$  is the sum (or union) of the spectral data of the restricted parts. In particular, since  $\mathcal{H}_\omega = \overline{\mathcal{H}_\omega}$ , the eigenvalues of the corresponding restrictions are equal and thus each eigenvalue of the restriction  $H_\omega = H|_{\mathcal{H}_\omega}$  enters the spectrum of  $H$  with multiplicity two. Kinematically, these eigenvalues correspond to the rotational wobbles of the antenna beam.

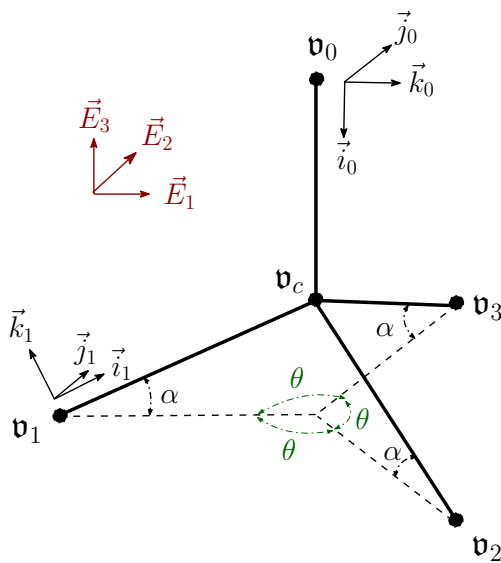


FIGURE 8. Geometry of three dimensional star graph in its equilibrium state.

*Proof of Theorem 5.1.* The graph  $\Gamma$  is invariant under the following geometric transformations and their products:  $R$  acting as the rotation counterclockwise by  $\theta = 2\pi/3$  around the axis  $-\vec{i}_0$ , and  $F$  acting as the reflection with respect to the plane spanned by  $\vec{i}_1$  and  $\vec{i}_0$ . These transformations generate the group  $G = D_3$ , the dihedral group<sup>7</sup> of degree 3, according to the presentation

$$G = \langle R, F \mid R^3 = I, F^2 = I, FRFR = I \rangle. \quad (80)$$

<sup>7</sup>It is isomorphic to the symmetric group  $S_3$  of permutations of 3 elements.

Let us now fix the following local bases: take  $\vec{j}_1$  to be orthogonal to the plane spanned by  $\vec{i}_0$  and  $\vec{i}_1$ ; let  $\vec{j}_0 = \vec{j}_1$ , see Figure 8; this determines  $\vec{k}_0$  and  $\vec{k}_1$ . More specifically,

$$\vec{i}_0 = \begin{pmatrix} 0 \\ 0 \\ -1 \end{pmatrix}, \quad \vec{j}_0 = \begin{pmatrix} 0 \\ 1 \\ 0 \end{pmatrix}, \quad \vec{k}_0 = \begin{pmatrix} 1 \\ 0 \\ 0 \end{pmatrix}, \quad \vec{i}_1 = \begin{pmatrix} \cos(\alpha) \\ 0 \\ \sin(\alpha) \end{pmatrix}, \quad \vec{j}_1 = \begin{pmatrix} 0 \\ 1 \\ 0 \end{pmatrix}, \quad \vec{k}_1 = \begin{pmatrix} -\sin(\alpha) \\ 0 \\ \cos(\alpha) \end{pmatrix}. \quad (81)$$

We also assume

$$\vec{i}_2 = R\vec{i}_1, \quad \vec{j}_2 = R\vec{j}_1, \quad \vec{k}_2 = R\vec{k}_1, \quad \text{and} \quad \vec{i}_3 = R\vec{i}_2, \quad \vec{j}_3 = R\vec{j}_2, \quad \vec{k}_3 = R\vec{k}_2. \quad (82)$$

With these choices, we obtain the following geometric representation<sup>8</sup> of  $G$ ,

$$R = \begin{pmatrix} \cos(\theta) & -\sin(\theta) & 0 \\ \sin(\theta) & \cos(\theta) & 0 \\ 0 & 0 & 1 \end{pmatrix}, \quad F = \begin{pmatrix} 1 & 0 & 0 \\ 0 & -1 & 0 \\ 0 & 0 & 1 \end{pmatrix}. \quad (83)$$

We now have to describe the action of  $G$  on the functions  $\{v_e, w_e, u_e, \eta_e\}$  defined along the beams  $e$  of the frame. We note that the space transformation  $T$  maps a vector  $\vec{g}$  based at a material point  $\vec{x}$  to the vector  $T\vec{g}$  at the point  $T\vec{x}$ . Therefore

$$R : \begin{pmatrix} \vec{g}_0 \\ \vec{g}_1 \\ \vec{g}_2 \\ \vec{g}_3 \end{pmatrix} \mapsto \begin{pmatrix} R\vec{g}_0 \\ R\vec{g}_3 \\ R\vec{g}_1 \\ R\vec{g}_2 \end{pmatrix} \quad \text{and} \quad F : \begin{pmatrix} \vec{g}_0 \\ \vec{g}_1 \\ \vec{g}_2 \\ \vec{g}_3 \end{pmatrix} \mapsto \begin{pmatrix} F\vec{g}_0 \\ F\vec{g}_1 \\ F\vec{g}_3 \\ F\vec{g}_2 \end{pmatrix} \quad (84)$$

On the other hand a transformation  $\mathcal{R}$  based at a point  $\vec{x}$  gets mapped to  $T\mathcal{R}T^{-1}$  at the point  $T\vec{x}$ . By direct calculation from definition (5) (or by using geometric intuition), we obtain that

$$R : \begin{pmatrix} \eta_0 \\ \eta_1 \\ \eta_2 \\ \eta_3 \end{pmatrix} \mapsto \begin{pmatrix} \eta_0 \\ \eta_3 \\ \eta_1 \\ \eta_2 \end{pmatrix} \quad \text{and} \quad F : \begin{pmatrix} \eta_0 \\ \eta_1 \\ \eta_2 \\ \eta_3 \end{pmatrix} \mapsto \begin{pmatrix} -\eta_0 \\ -\eta_1 \\ -\eta_3 \\ -\eta_2 \end{pmatrix}. \quad (85)$$

Since, by definition,  $\vec{g}_n = u_n\vec{i}_n + w_n\vec{j}_n + v_n\vec{k}_n$ , mapping rules (84) and (85) induce the linear action of  $R$  and  $F$  on the space  $L^2(\Gamma)$ . These linear actions commute with the operator  $H$  (in particular, preserving its domain) and form a representation of the group  $G$ .

It is well-known [34, 15] that the Hilbert space  $L^2(\Gamma)$  with an action of a finite group  $G$  on it can be decomposed into a sum of **isotypic components**, i.e. the subspaces consisting of all copies of a given irreducible representation (**irrep**) contained in  $L^2(\Gamma)$ . Concretely, if  $\rho$  is an irrep with character  $\chi_\rho : G \rightarrow \mathbb{C}$ , then

$$\mathbf{P}_\rho = \frac{\dim \rho}{|G|} \sum_{g \in G} \overline{\chi_\rho(g)} g \quad (86)$$

is the orthogonal projector onto the isotypic component of  $\rho$ , see [15, Equation (2.32)]. Here  $\dim \rho$  is the dimension of the representation and the last  $g$  should be understood as the representative of the group element acting on the Hilbert space in question. It is a classical result of representation theory that the projectors  $\mathbf{P}_\rho$  corresponding to different irreps are mutually orthogonal and their sum over all irreps of  $G$  is identity. Since  $H$  commutes with every  $g \in G$ , the projector  $\mathbf{P}_\rho$  commutes with  $H$  and therefore the subspace  $\mathbf{P}_\rho(L^2(\Gamma))$  is reducing.

<sup>8</sup>With a slight abuse of notation we use the same letters for the group elements and the matrices realizing their action on the corresponding linear space

Our group  $G = D_3$  has three irreducible representations, known as trivial (identity), alternating and standard. The first two are one-dimensional and the last one is two-dimensional. We will denote the corresponding isotypic components by  $\mathcal{H}_{\text{trv}}$ ,  $\mathcal{H}_{\text{alt}}$  and  $\mathcal{H}_{\text{std}}$ . The group  $D_3$  contains the cyclic group  $C_3$  as a subgroup; it is generated by the rotations  $R$ ,

$$C_3 = \langle R \mid R^3 = I \rangle \subset D_3. \quad (87)$$

The group  $C_3$  also have three representations: identity,  $\omega = e^{2\pi i/3}$ , and  $\bar{\omega}$ , all one-dimensional.

The character of the standard representation of  $D_3$  is non-zero only on the elements of  $C_3 \subset D_3$ , more precisely,

$$\chi_{\text{std}}(g) = \begin{cases} \chi_{\omega}(g) + \chi_{\bar{\omega}}(g), & g \in C_3, \\ 0, & g \notin C_3, \end{cases} \quad (88)$$

which gives

$$\mathbf{P}_{\text{std}} = \frac{2}{|D_3|} \sum_{g \in D_3} \overline{\chi_{\text{std}}(g)} g = \frac{1}{|C_3|} \sum_{g \in C_3} \left( \overline{\chi_{\omega}(g)} + \overline{\chi_{\bar{\omega}}(g)} \right) g = \mathbf{P}_{\omega} + \mathbf{P}_{\bar{\omega}}. \quad (89)$$

This, together with observation that  $\chi_{\bar{\omega}} = \overline{\chi_{\omega}(g)}$  and therefore  $\mathbf{P}_{\bar{\omega}} = \overline{\mathbf{P}_{\omega}}$ , proves decomposition (76) in principle. To specify details of the individual spaces as in equations (77)–(79), we can proceed by definition, computing the ranges of the corresponding projectors  $\mathbf{P}_{\text{trv}}$ ,  $\mathbf{P}_{\text{alt}}$  and  $\mathbf{P}_{\omega}$  using equation (86). This requires summation over  $|D_3| = 6$  or  $|C_3| = 3$  group elements and is rather tedious.

Instead we will use the fact that all representations are one-dimensional and therefore the isotypic components are isomorphic to the corresponding spaces of **intertwiners**.<sup>9</sup> Recall the following definition: let  $G$  be a finite group with two representations  $\rho : G \rightarrow \text{GL}(V_{\rho})$  and  $\sigma : G \rightarrow \text{GL}(V_{\sigma})$ . The vector space homomorphism  $\phi : V_{\rho} \rightarrow V_{\sigma}$  is said to be an **intertwiner** if it satisfies

$$\forall g \in G, \quad \sigma(g)\phi = \phi\rho(g). \quad (90)$$

The vector space of all intertwiners is denoted by  $\text{Hom}_G(V_{\rho}, V_{\sigma})$ .

In our setting  $V_{\sigma}$  is  $L^2(\Gamma)$  with the action of  $G$  defined by (84)–(85);  $\rho$  will be one of the irreps of  $G$ . Since we only deal with 1-dimensional representations (i.e.  $\rho(g)$  is a scalar),  $\phi$  are simply the eigenvectors of  $R$  and  $F$  on  $L^2(\Gamma)$ . The detailed calculations are performed in the next three sections.  $\square$

5.3.1. *Trivial irrep.* We first consider the trivial (identity) irreducible representation  $\rho = \text{trv}$  of  $D_3$ , given by  $V_{\rho} = \mathbb{C}^1$ ,  $\rho(R) = 1$ , and  $\rho(F) = 1$ . We will now use intertwiner condition (90) to calculate the intertwiners which are just vectors from  $L^2(\Gamma)$ . Naturally, it is enough to check condition (90) only on the generators of the group.

Applying the intertwiner condition to  $R$  from (84), we have

$$R \begin{pmatrix} \vec{g}_0 \\ \vec{g}_1 \\ \vec{g}_2 \\ \vec{g}_3 \end{pmatrix} = \begin{pmatrix} R\vec{g}_0 \\ R\vec{g}_3 \\ R\vec{g}_1 \\ R\vec{g}_2 \end{pmatrix} = \begin{pmatrix} \vec{g}_0 \\ \vec{g}_1 \\ \vec{g}_2 \\ \vec{g}_3 \end{pmatrix} \cdot 1,$$

---

<sup>9</sup>The action of an operator on the space of intertwiners is somewhat different from its action on the isotypic component and results in a decomposition with some favorable spectral properties [2]. However the two notions coincide for a one-dimensional representation.

in particular  $R\vec{g}_0 = \vec{g}_0$ , which means that for any  $x$ ,  $\vec{g}_0(x)$  is proportional to the eigenvector of  $R$  with eigenvalue 1, see (83) and therefore

$$v_0 \equiv 0 \quad \text{and} \quad w_0 \equiv 0. \quad (91)$$

We also have  $R\vec{g}_1 = \vec{g}_2$  and  $R\vec{g}_2 = \vec{g}_3$  yielding, since  $R$  is orthogonal,

$$u_2 := \vec{i}_2 \cdot \vec{g}_2 = (R\vec{i}_1) \cdot (R\vec{g}_1) = \vec{i}_1 \cdot \vec{g}_1 = u_1,$$

and so on,

$$v_1 = v_2 = v_3, \quad w_1 = w_2 = w_3 \quad \text{and} \quad u_1 = u_2 = u_3. \quad (92)$$

Switching our attention to  $F$ , we have from equation (84)

$$w_1 := \vec{j}_1 \cdot \vec{g}_1 = \vec{j}_1 \cdot (F\vec{g}_1) = (F\vec{j}_1) \cdot \vec{g}_1 = -\vec{j}_1 \cdot \vec{g}_1 = -w_1,$$

and thus

$$w_1 = w_2 = w_3 \equiv 0. \quad (93)$$

Finally, equation (85) gives

$$F \begin{pmatrix} \eta_0 \\ \eta_1 \\ \eta_2 \\ \eta_3 \end{pmatrix} = \begin{pmatrix} -\eta_0 \\ -\eta_1 \\ -\eta_3 \\ -\eta_2 \end{pmatrix} = \begin{pmatrix} \eta_0 \\ \eta_1 \\ \eta_2 \\ \eta_3 \end{pmatrix},$$

therefore all torsion fields are identically zero,

$$\eta_1 = \eta_2 = \eta_3 \equiv 0. \quad (94)$$

It is an easy check that the remaining conditions result in no additional restrictions on the undetermined  $u_0$ ,  $u$  and  $v$ , where we abbreviated  $u := u_s$  and  $v := v_s$  for  $s = 1, 2, 3$ . The conditions we obtained describe the space  $\mathcal{H}_{\text{trv}}$ .

We now describe the *domain* of the operator  $H_{\text{trv}} := H|_{\mathcal{H}_{\text{trv}}}$ . First of all, the functions  $u_0$ ,  $u$  and  $v$  need to come from Sobolev spaces  $H^2(0, \ell_0)$ ,  $H^2(0, \ell)$  and  $H^4(0, \ell)$  correspondingly. Continuity of displacement (35) at the central joint becomes

$$u(\ell)\vec{i}_1 + v(\ell)\vec{k}_1 = u_0(\ell_0)\vec{i}_0. \quad (95)$$

Expressing  $\vec{i}_0$  in the local coordinate system of  $e_1$ , i.e.

$$\vec{i}_0 = -\sin(\alpha)\vec{i}_1 - \cos(\alpha)\vec{k}_1 \quad (96)$$

implies that at vertex  $c$  the relations

$$u(\ell) + u_0(\ell_0)\sin(\alpha) = 0, \quad v(\ell) + u_0(\ell_0)\cos(\alpha) = 0 \quad (97)$$

should be satisfied. Using (91), (92) and (93) in (36), we get

$$v'(\ell) = 0. \quad (98)$$

Similarly, the balance of forces, equation (37), reduces to

$$av'''(\ell)(\vec{k}_1 + \vec{k}_2 + \vec{k}_3) + cu'(\ell)(\vec{i}_1 + \vec{i}_2 + \vec{i}_3) + cu'_0(\ell_0)\vec{i}_0 = 0$$

Applying identities  $\vec{i}_1 + \vec{i}_2 + \vec{i}_3 = -3\vec{i}_0\sin(\alpha)$  and  $\vec{k}_1 + \vec{k}_2 + \vec{k}_3 = -3\vec{i}_0\cos(\alpha)$ , it takes the form

$$3av'''(\ell)\cos(\alpha) + 3cu'(\ell)\sin(\alpha) - c_0u'_0(\ell_0) = 0 \quad (99)$$

Finally, due to (93), (94) and  $\vec{j}_1 + \vec{j}_2 + \vec{j}_3 = 0$ , the balance of moments condition (38) will be automatically satisfied.

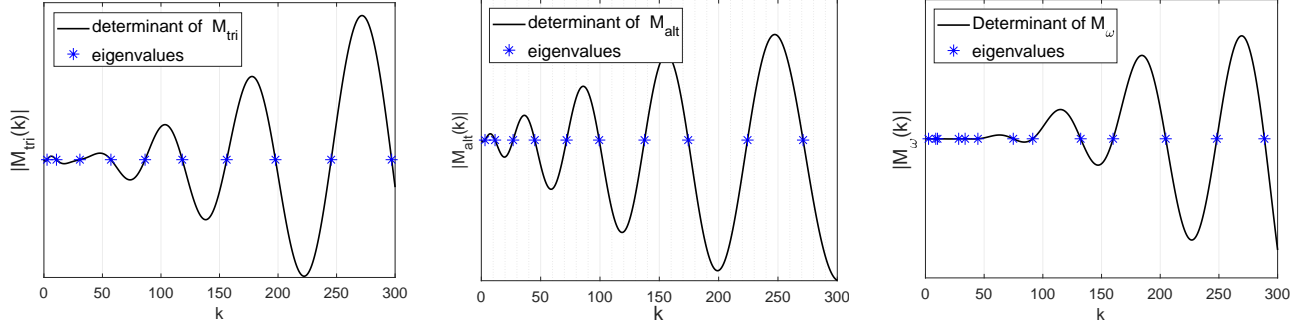


FIGURE 9. Variation of determinant of matrices corresponding irreducible representations and their corresponding eigenvalues: (left) trivial  $M_{\text{trv}}$ , (middle) alternating  $M_{\text{alt}}$ , and (right) standard  $M_{\omega}$ . All the results are based on unit materials parameters and beams lengths.

The fixed end at  $\mathbf{v}_1$  results in conditions

$$u(0) = v(0) = v'(0) = 0, \quad (100)$$

while free end at  $\mathbf{v}_0$  gives

$$u'_0(0) = 0. \quad (101)$$

The eigenproblem for the operator  $H_{\text{trv}}$  becomes

$$a \frac{d^4 v(x)}{dx^4} = \lambda v(x), \quad c \frac{d^2 u(x)}{dx^2} = \lambda u(x), \quad c_0 \frac{d^2 u_0(x)}{dx^2} = \lambda u_0(x) \quad (102)$$

together with conditions (97), (98), (99), (100) and (101).

Imposing conditions (100) and (101) first, we get

$$v(x) = A(\sinh(\mu_a x) - \sin(\mu_a x)) + B(\cosh(\mu_a x) - \cos(\mu_a x)) \quad (103)$$

and

$$u(x) = C \sin(\beta_c x), \quad u_0(x) = D \cos(\beta_{c_0} x) \quad (104)$$

where  $\mu_a := (\lambda/a)^{1/4}$ ,  $\beta_d := (\lambda/d)^{1/2}$  and  $\beta_{c_0} := (\lambda/c_0)^{1/2}$ . Application of conditions (97), (98) and (99) brings us to the equivalent problem of finding non-trivial coefficient vector  $(A \ B \ C \ D)^T$  in the kernel of the matrix  $M_{\text{trv}} = M_{\text{trv}}(\lambda)$  defined as (see (75) for the definition of notations)

$$M_{\text{trv}}(\lambda) = \begin{pmatrix} C_{\mu_a \ell}^- & S_{\mu_a \ell}^+ & 0 & 0 \\ 0 & 0 & S_{\beta_c \ell} & S_{\alpha} C_{\beta_{c_0} \ell_0} \\ S_{\mu_a \ell}^- & C_{\mu_a \ell}^- & 0 & C_{\alpha} C_{\beta_{c_0} \ell_0} \\ 3a\mu_a^3 C_{\alpha} C_{\mu_a \ell}^+ & 3a\mu_a^3 C_{\alpha} S_{\mu_a \ell}^- & 3c\beta_c S_{\alpha} C_{\beta_c \ell} & c_0\beta_{c_0} S_{\beta_{c_0} \ell_0} \end{pmatrix}.$$

The eigenvalues  $\lambda$  are determined as the points in which  $\det(M_{\text{trv}}) = 0$ .

**Example 1.** We set all material constants and beam lengths to 1. Figure 9(left) plots the value of  $\det(M_{\text{trv}})$ . Figure 10 shows the components of the first eigenfunction corresponding to the trivial representation. For verification purposes, the latter plot was obtained from finite-element calculation for the *entire structure*, without symmetry reduction, i.e. without enforcing conditions (91)–(94). Thus we can confirm by a different method that the relevant fields are zero (up to a numerical error).

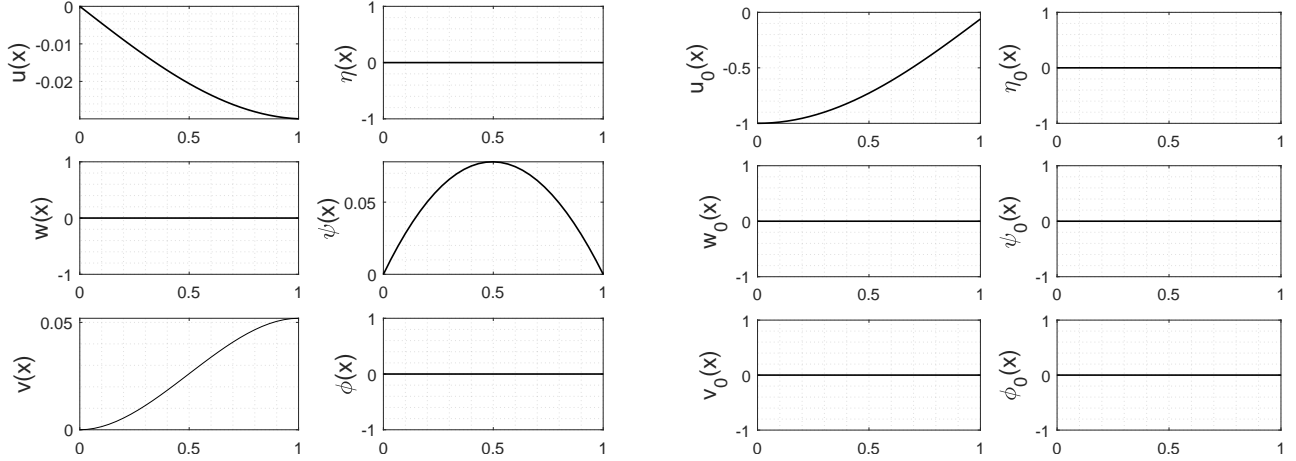


FIGURE 10. Plot of the components of the first eigenfunction from  $\mathcal{H}_{\text{trv}}$ . Plots are obtained from a finite elements numerical computation and are displayed in the local coordinate system of the corresponding edge. All the results are based on unit materials parameters and beams lengths.

5.3.2. *Alternating irrep.* For the alternating representation,  $\rho(R) = 1$  and  $\rho(F) = -1$ . Identities (91) and (92) still apply in this case, and we also have from equation (85)(left)

$$\eta_1 = \eta_2 = \eta_3 =: \eta. \quad (105)$$

Turning to  $F$ , condition  $F\vec{g}_0 = -\vec{g}_0$  yields

$$u_0 \equiv 0 \quad (106)$$

(in addition to  $v_0 = w_0 \equiv 0$  we already have), while  $F\vec{g}_1 = -\vec{g}_1$  gives

$$u_1 := \vec{i}_1 \cdot \vec{g}_1 = -\vec{i}_1 \cdot (F\vec{g}_1) = -(F\vec{i}_1) \cdot \vec{g}_1 = -\vec{i}_1 \cdot \vec{g}_1 = -u_1,$$

and, similarly,  $v_1 = -v_1$ , therefore

$$u_1 = u_2 = u_3 \equiv 0 \quad \text{and} \quad v_1 = v_2 = v_3 \equiv 0. \quad (107)$$

Condition (85)(right) results in no further restrictions. We have arrived to (78) and the problem is fully described in terms of remaining degrees of freedom  $\eta_0$ ,  $w$  and  $\eta$ .

We will now describe the domain of the operator  $H_{\text{alt}} := H|_{\mathcal{H}_{\text{alt}}}$ . Identities (91), (106) and (107) reduce the displacement continuity to

$$w(\ell) = 0. \quad (108)$$

Using (96) and the continuity of rotation reduces to

$$\eta(\ell) + \eta_0(\ell_0) \sin(\alpha) = 0, \quad w'(\ell) + \eta_0(\ell_0) \cos(\alpha) = 0. \quad (109)$$

Balance of forces, equation (37) becomes  $bw'''(\ell)(\vec{j}_1 + \vec{j}_2 + \vec{j}_3) = 0$ , which is satisfied automatically due to  $\vec{j}_1 + \vec{j}_2 + \vec{j}_3 = 0$ . Finally, balance of moments, equation (38), takes the form

$$-bw''(\ell)(\vec{k}_1 + \vec{k}_2 + \vec{k}_3) + d\eta'(\ell)(\vec{i}_1 + \vec{i}_2 + \vec{i}_3) + d\eta'_0(\ell_0) = 0,$$

and, via identities  $\vec{i}_1 + \vec{i}_2 + \vec{i}_3 = -3\vec{i}_0 \sin(\alpha)$  and  $\vec{k}_1 + \vec{k}_2 + \vec{k}_3 = -3\vec{i}_0 \cos(\alpha)$ , reduces to

$$3bw''(\ell) \cos(\alpha) - 3d\eta'(\ell) \sin(\alpha) + d_0\eta'_0(\ell_0) = 0. \quad (110)$$

The conditions at the degree 1 endpoints result in

$$\eta(0) = w(0) = w'(0) = 0 \quad \text{and} \quad \eta'_0(0) = 0. \quad (111)$$

Solving the eigenvalue equations and imposing endpoint conditions (111) results in

$$w(x) = A(\sinh(\mu_b x) - \sin(\mu_b x)) + B(\cosh(\mu_b x) - \cos(\mu_b x))$$

and

$$\eta(x) = C \sin(\beta_d x), \quad \eta_0(x) = D \cos(\beta_{d_0} x)$$

where  $\mu_b = (\lambda/b)^{1/4}$ ,  $\beta_d = (\lambda/d)^{1/2}$  and  $\beta_{d_0} = (\lambda/d_0)^{1/2}$ . Applying the vertex conditions (108), (109) and (110), the eigenvalue problem reduces to condition  $\det(M_{\text{alt}}(\lambda)) = 0$ , where

$$M_{\text{alt}}(\lambda) = \begin{pmatrix} S_{\mu_b \ell}^- & C_{\mu_b \ell}^- & 0 & 0 \\ 0 & 0 & S_{\beta_d \ell} & S_{\alpha} C_{\beta_{d_0} \ell_0} \\ \mu_b C_{\mu_b \ell}^- & \mu_b S_{\mu_b \ell}^+ & 0 & C_{\alpha} C_{\beta_{d_0} \ell_0} \\ 3b\mu_b^2 C_{\alpha} S_{\mu_b \ell}^+ & 3b\mu_b^2 C_{\alpha} C_{\mu_b \ell}^+ & -3\mu d S_{\alpha} C_{\beta_d \ell} & -d_0 \beta_{d_0} S_{\beta_{d_0} \ell_0} \end{pmatrix}.$$

**Example 2.** Continuing Example 1, Figure 9(middle) plots the determinant of the matrix  $M_{\text{alt}}$  with the roots highlighted. Figure 11 shows the components of the eigenfunction corresponding to the first eigenvalue of alternating representation.

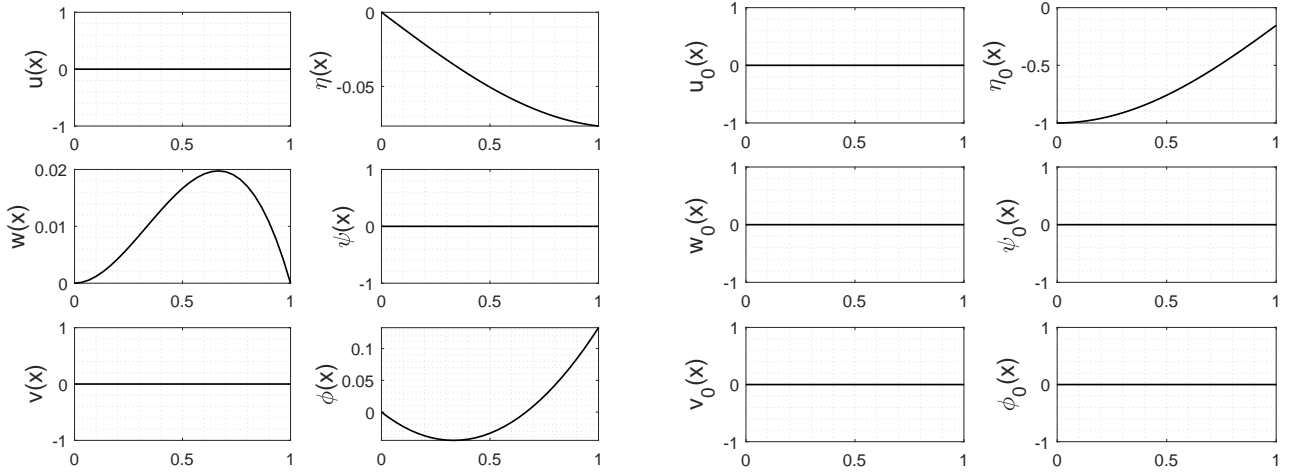


FIGURE 11. Plot of the components of the first eigenfunction from  $\mathcal{H}_{\text{alt}}$ . Plots are obtained from a finite elements numerical computation and are displayed in the local coordinate system of the corresponding edge. All the results are based on unit materials parameters and beams lengths.

5.3.3. *Irrep  $\omega$  of  $C_3$ .* To derive the description of  $\mathcal{H}_\omega$ , we only have the conditions

$$\begin{pmatrix} R\vec{g}_0 \\ R\vec{g}_3 \\ R\vec{g}_1 \\ R\vec{g}_2 \end{pmatrix} = \omega \begin{pmatrix} \vec{g}_0 \\ \vec{g}_1 \\ \vec{g}_2 \\ \vec{g}_3 \end{pmatrix} \quad \text{and} \quad \begin{pmatrix} \eta_0 \\ \eta_3 \\ \eta_1 \\ \eta_2 \end{pmatrix} = \omega \begin{pmatrix} \eta_0 \\ \eta_1 \\ \eta_2 \\ \eta_3 \end{pmatrix}, \quad (112)$$

obtained by applying  $\rho(R) = \omega := e^{2\pi i/3}$  to (90), (84) and (85).

For beam  $e_0$  we have

$$u_0 = 0, \quad \eta_0 = 0, \quad w_0 = iv_0, \quad (113)$$



while on the other beams,

$$v_2 = \omega v_1, \quad w_2 = \omega w_1, \quad u_2 = \omega u_1, \quad \eta_2 = \omega \eta_1, \quad (114)$$

$$v_3 = \bar{\omega} v_1, \quad w_3 = \bar{\omega} w_1, \quad u_3 = \bar{\omega} u_1, \quad \eta_3 = \bar{\omega} \eta_1. \quad (115)$$

Displacement continuity, equation (35), for the edges  $e_1$  and  $e_0$  has the form

$$u(\ell)\vec{i}_1 + w(\ell)\vec{j}_1 + v(\ell)\vec{k}_1 = w_0(\ell_0)\vec{j}_0 + v_0(\ell_0)\vec{k}_0,$$

where, as before, we abbreviated  $(v, w, u, \eta) := (v_1, w_1, u_1, \eta_1)$ . Applying  $\vec{j}_0 = \vec{j}_1$  and  $\vec{k}_0 = \cos(\alpha)\vec{i}_1 - \sin(\alpha)\vec{k}_1$  (see Figure 8) and equation (113), the vertex condition reduces to

$$u(\ell) - v_0(\ell_0) \cos(\alpha) = 0, \quad v(\ell) + v_0(\ell_0) \sin(\alpha) = 0, \quad w(\ell) - iv_0(\ell_0) = 0 \quad (116)$$

Simple calculations show that same relations as (116) holds by replacing  $e_1$  with  $e_2$  or  $e_3$ .

Rotation continuity, equation (36), becomes

$$\eta(\ell)\vec{i}_1 - v'(\ell)\vec{j}_1 + w'(\ell)\vec{k}_1 = -v'_0(\ell_0)\vec{j}_0 + w'_0(\ell_0)\vec{k}_0,$$

similarly leading to

$$\eta(\ell) - iv'_0(\ell_0) \cos(\alpha) = 0, \quad w'(\ell) + iv'_0(\ell_0) \sin(\alpha) = 0, \quad v'(\ell) - v'_0(\ell_0) = 0. \quad (117)$$

The vertex condition (37) reduces to

$$\begin{aligned} cu'(\ell)(\vec{i}_1 + \omega\vec{i}_2 + \bar{\omega}\vec{i}_3) - bw'''(\ell)(\vec{j}_1 + \omega\vec{j}_2 + \bar{\omega}\vec{j}_3) \\ - av'''(\ell)(\vec{k}_1 + \omega\vec{k}_2 + \bar{\omega}\vec{k}_3) - b_0w_0'''(\ell_0)\vec{j}_0 - a_0v_0'''(\ell_0)\vec{k}_0 = 0. \end{aligned} \quad (118)$$

Identities

$$\vec{i}_1 + \omega\vec{i}_2 + \bar{\omega}\vec{i}_3 = \frac{3}{2} \begin{pmatrix} \cos(\alpha) \\ i \cos(\alpha) \\ 0 \end{pmatrix}, \quad \vec{j}_1 + \omega\vec{j}_2 + \bar{\omega}\vec{j}_3 = \frac{3}{2} \begin{pmatrix} -i \\ 1 \\ 0 \end{pmatrix}, \quad \vec{k}_1 + \omega\vec{k}_2 + \bar{\omega}\vec{k}_3 = -\frac{3}{2} \begin{pmatrix} \sin(\alpha) \\ i \sin(\alpha) \\ 0 \end{pmatrix}$$

and  $\vec{j}_0 = (0 \ 1 \ 0)^T$ ,  $\vec{k}_0 = (1 \ 0 \ 0)^T$ ,  $a_0 = b_0$  reduce equation (118) to a single linearly independent condition, namely

$$\frac{3}{2}cu'(\ell) \cos(\alpha) + \frac{3}{2}biw'''(\ell) + \frac{3}{2}av'''(\ell) \sin(\alpha) - a_0v_0'''(\ell_0) = 0. \quad (119)$$

The vertex condition (38) reduces to

$$\begin{aligned} d\eta'(\ell)(\vec{i}_1 + \omega\vec{i}_2 + \bar{\omega}\vec{i}_3) - av''(\ell)(\vec{j}_1 + \omega\vec{j}_2 + \bar{\omega}\vec{j}_3) \\ + bw''(\ell)(\vec{k}_1 + \omega\vec{k}_2 + \bar{\omega}\vec{k}_3) - a_0v_0''(\ell_0)\vec{j}_0 + b_0w_0''(\ell_0)\vec{k}_0 = 0, \end{aligned}$$

which is equivalent to single equation

$$\frac{3}{2}d\eta'(\ell) \cos(\alpha) - \frac{3}{2}biw''(\ell) \sin(\alpha) - \frac{3}{2}av''(\ell) - a_0v_0''(\ell_0) = 0. \quad (120)$$

With the restrictions given by (113) and (114), the eigenvalue problem is fully determined by functions  $v, w, u$  and  $\eta$  on the base edges and the function  $v_0$  defined on vertical edge. Solving the

corresponding differential equations and imposing free vertex condition at  $\mathbf{v}_0$  and clamped vertex conditions at  $\mathbf{v}_1$ ,  $\mathbf{v}_2$ , and  $\mathbf{v}_3$ , the general solutions can be written as

$$\begin{aligned} v(x) &= A(\sinh(\mu x) - \sin(\mu x)) + B(\cosh(\mu x) - \cos(\mu x)) \\ i\omega(x) &= C(\sinh(\mu x) - \sin(\mu x)) + D(\cosh(\mu x) - \cos(\mu x)) \\ u(x) &= E \sin(\beta x), \\ i\eta(x) &= F \sin(\beta x) \\ v_0(x) &= A_0(\sinh(\mu_0 x) + \sin(\mu_0 x)) + B_0(\cosh(\mu_0 x) + \cos(\mu_0 x)) \end{aligned}$$

where  $\mu = \lambda^{1/4}$ ,  $\beta = \lambda^{1/2}$ ,  $\mu_0 = (\lambda/a_0)^{1/4}$ , and  $\beta_0 = (\lambda/a_0)^{1/2}$ .

Applying vertex conditions (116), (117), (119), and (120), we reduce the eigenvalue problem to an equation of the form  $\det(M_\omega(\lambda)) = 0$ . If we make additional simplifying assumptions that  $a_0 = a = b = c = 1$  the matrix  $M_\omega(\lambda)$  becomes

$$M_\omega(\lambda) = \begin{pmatrix} C_{\mu\ell}^- & S_{\mu\ell}^- & 0 & 0 & 0 & 0 & -C_{\mu\ell_0}^+ & -S_{\mu\ell_0}^- \\ 0 & 0 & S_{\mu\ell}^- & C_{\mu\ell}^- & 0 & 0 & S_{\mu\ell_0}^+ & C_{\mu\ell_0}^+ \\ 0 & 0 & 0 & 0 & S_{\beta\ell} & 0 & -C_\alpha S_{\mu\ell_0}^+ & -C_\alpha C_{\mu\ell_0}^+ \\ 0 & 0 & 0 & 0 & 0 & S_{\beta\ell} & \mu C_\alpha C_{\mu\ell_0}^+ & \mu C_\alpha S_{\mu\ell_0}^- \\ S_{\mu\ell}^- & C_{\mu\ell}^- & 0 & 0 & 0 & 0 & S_\alpha S_{\mu\ell_0}^+ & S_\alpha C_{\mu\ell_0}^+ \\ 0 & 0 & C_{\mu\ell}^- & S_{\mu\ell}^+ & 0 & 0 & -S_\alpha C_{\mu\ell_0}^+ & -S_\alpha S_{\mu\ell_0}^- \\ \frac{3\mu}{2} S_\alpha C_{\mu\ell}^+ & \frac{3\mu}{2} S_\alpha S_{\mu\ell}^- & \frac{3\mu}{2} C_{\mu\ell}^+ & \frac{3\mu}{2} S_{\mu\ell}^- & \frac{3}{2} C_\alpha C_{\beta\ell} & 0 & -\mu C_{\mu\ell_0}^- & -\mu S_{\mu\ell_0}^+ \\ -\frac{3}{2} S_{\mu\ell}^+ & -\frac{3}{2} C_{\mu\ell}^+ & -\frac{3}{2} S_\alpha S_{\mu\ell}^+ & -\frac{3}{2} S_\alpha C_{\mu\ell}^+ & 0 & \frac{3}{2} C_\alpha C_{\beta\ell} & -S_{\mu\ell_0}^- & -C_{\mu\ell_0}^- \end{pmatrix},$$

**Example 3.** Continuing Example 1, Figure 9(right) plots the  $\det(M_\omega)$  with the roots highlighted. Figure 12 shows the components of the *real part* of the eigenfunction corresponding to the first eigenvalue of  $\omega$  representation of  $C_3$ . The real part is an eigenfunction of the original problem because if  $\Psi$  is an eigenfunction in  $\mathcal{H}_\omega$ , then  $\bar{\Psi}$  is an eigenfunction in  $\mathcal{H}_{\bar{\omega}}$  with the same eigenvalue.

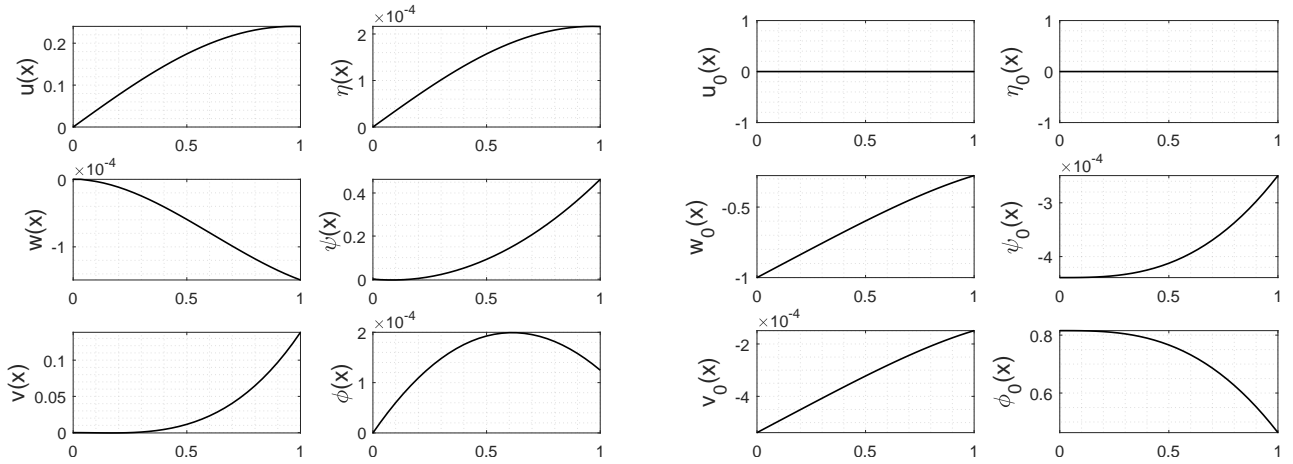


FIGURE 12. Plot of (first) eigenfunction fields corresponding to the eigenvalue of multiplicity two in edge's local coordinate system by finite element approximation. All the results are based on unit value of materials properties and unit beam's lengths.

Additionally, we display in Figure 13 a visualization of the two independent eigenfunctions from  $\mathcal{H}_\omega \oplus \mathcal{H}_{\bar{\omega}}$ .

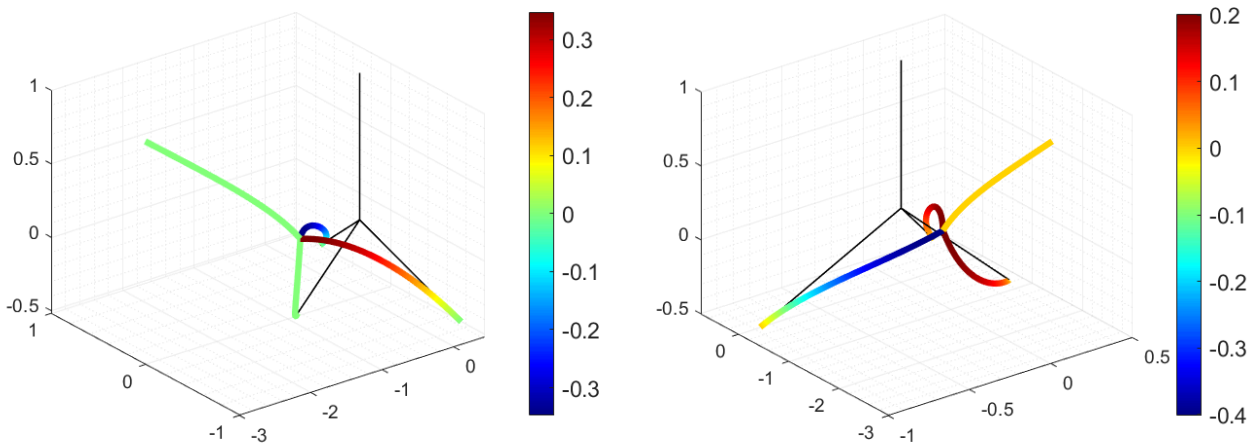


FIGURE 13. Plot of the first and second eigenfunctions corresponding to the standard representation in global coordinate system. The results are obtained by a finite element approximation of the entire structure with 20 number of element for each beam. The angle  $\alpha = \pi/6$ , and unit values for all material's parameters and beam's lengths are selected. The eigenvalues agree up to order  $10^{-8}$  due to finite number of discretization elements.

## 6. OUTLOOK

In this section we give a partial list of topics that would benefit from the spectral-theoretic approach. The most obvious is to extend our results to Timoshenko beams. Timoshenko model no longer assumes the cross-sections remain orthogonal to the deformed axis and therefore incorporates more degrees of freedom [30, 39, 16, 37].

Of similar applied interest is the analysis of pre-curved beams which play an important role in application of highly flexible thin structures. Such beams may exhibit unusual and unexpected behavior, and their spectral analysis does not seem to be explored fully. Along this applied path, extension of the current framework to the case of semi-rigid joints, as well as the case of concentrated masses carried by them may be interesting to the community (see, for example, [31, 9, 10, 19, 48, 17] and references therein).

The viability of the frame model as a structure composed of one-dimensional segments also needs to be verified mathematically, as a limit of a three-dimensional structure as the beam widths are going to zero. This approach will also be of interest to structural engineers working with FEM-packages for 3-D structural elements such as Kirchhoff–Love plates. There is a significant mathematical literature on this question for second-order operators (see, for example, [26, 53, 18, 43]), with some recent advances for the fourth-order operators [13, 32, 33]. Of particular interest may be the approach via general scales of quadratic forms [41, 44] which can be more readily adapted to the present setting. A variety of operators may be expected to arise in the limit, including the operators with masses concentrating at joints and other cases of applied interest.

Going in the other direction, it is interesting to investigate the limit of the operator we discussed when some material parameters are either very small or very large. For example, consider taking

the angular displacement stiffness  $d$  to 0 or to  $\infty$  in the planar case. In both limits the out-of-plane displacement  $v$  can be expected to decouple from the rest of the degrees of freedom, but with different vertex conditions at the joint (see [17] for a classification of self-adjoint conditions applicable to this case).

One of the methods to ease the computation of eigenvalues for beam frames is the Williams–Wittrick method [50, 51], which, in mathematical terms, uses a finite-rank perturbation to obtain a simpler system (decoupled beams) whose eigenvalues bound the eigenvalues of the original frame. Extending similar “graph surgery” methods summarized in [4] to the present setting would result in improved spectral estimates and answers to natural spectral optimization questions.

Many of the real-life beam structures are periodic; for those, Floquet–Bloch analysis [25, 54, 28] is a natural tool to understand the spectrum and to eventually design structures that block certain ranges of frequencies. Along the same line, spectral analysis of a fourth-order operator on periodic hexagonal lattices was recently discussed in [14].

Finally, the positivity of the ground state is a feature that is almost taken for granted in studies of the Laplacian and which is broken in the example shown in Figure 6. That fourth-order operators may have non-positive ground states is a well-known fact [47]. The positivity is restored when the angular displacement stiffness  $d$  is large (Figure 7), amplifying the second order part of the operator compared to the fourth order, see (54). A careful extension of the second-order theory on graphs [27] to the present case is thus sorely needed.

#### ACKNOWLEDGMENT

This work was partially supported by the NSF grant DMS-1815075 and BSF grant No. 2016281. The authors gratefully acknowledge enlightening discussions with and improving suggestions by Delio Mugnolo and Maryam Shakiba. Numerous insightful suggestions by the referees helped us improve the manuscript and give a more complete picture of the existing literature.

#### APPENDIX A. RODRIGUES’ ROTATION FORMULA.

Starting with the fact that  $\mathcal{R} \in \text{SO}(3)$ , then  $\mathcal{R}$  in (15) can be fully characterized by three free parameters, namely, axis of rotation represented by unit vector  $\vec{\vartheta}(x)$  and angle of rotation  $\alpha \in [0, \pi]$ . Let define skew-symmetric matrix  $\mathcal{K}$  with components

$$\mathcal{K}_{pq} = - \sum_{r=1}^3 \epsilon_{pqr} \vartheta_r, \quad p, q \in \{1, 2, 3\}, \quad (121)$$

where  $\vartheta_r$  is the  $r$ -th coordinate of the vector  $\vec{\vartheta}(x)$  in the global basis  $\{\vec{E}_1, \vec{E}_2, \vec{E}_3\}$ , and  $\epsilon_{pqr}$  is the Levi-Civita alternating symbol defined as the scalar triple product of orthonormal vectors in a right-handed system  $\{\vec{e}_1, \vec{e}_2, \vec{e}_3\}$  as  $\epsilon_{pqr} = \vec{e}_p \cdot (\vec{e}_q \times \vec{e}_r)$ . The operator  $\mathcal{R}$  corresponding to  $\vec{\vartheta}$  and  $\alpha$  then has a form

$$\mathcal{R}(x) = \mathbb{I} + (\sin \alpha) \mathcal{K}(x) + (1 - \cos \alpha) \mathcal{K}^2(x) \quad (122)$$

with  $\mathbb{I}$  is the  $3 \times 3$  identity matrix. Application of  $\mathcal{R}$  in (122) on vector  $\vec{a} \in \mathbb{R}^3$  will transform the vector to  $\vec{\mathbf{a}}$  of the form

$$\vec{\mathbf{a}} = \vec{a} \cos \alpha + (\vec{\vartheta} \times \vec{a}) \sin \alpha + \vec{\vartheta}(\vec{\vartheta} \cdot \vec{a})(1 - \cos \alpha) \quad (123)$$

which is the so-called Euler-Rodrigues formula. Replacing  $\vec{a}$  with  $\vec{i}$  in (123), then

$$\vec{i}(x) = \vec{i} \cos \alpha + (\vec{\vartheta}(x) \times \vec{i}) \sin \alpha + \vec{\vartheta}(x) (\vec{\vartheta}(x) \cdot \vec{i}) (1 - \cos \alpha) \quad (124)$$

For small deformation, let introduce (linearized)-rotation vector

$$\vec{\omega}(x) = \alpha \vec{\vartheta}(x) \quad (125)$$

Then the leading terms of (124), i.e., by neglecting terms of order  $\mathcal{O}(\alpha^2)$ , recovers (18). Similar discussion holds on recovering the leading terms in (19) and (20). Following Lemma establishes connection of (122) with the exponential form in (15).

**Lemma A.1.** *Rotational matrix  $\mathcal{R}$  in (122) with  $\mathcal{K}$  as (121) can be represented in exponential form  $\mathcal{R} = \exp(\Omega)$ , see (15), with  $\Omega = \alpha \mathcal{K}$ .*

**Proof of Lemma A.1.** Simple calculation on the components in (121) implies that matrix  $\mathcal{K}$  has the form

$$\mathcal{K} = \begin{pmatrix} 0 & -\vartheta_3 & \vartheta_2 \\ \vartheta_3 & 0 & -\vartheta_1 \\ -\vartheta_2 & \vartheta_1 & 0 \end{pmatrix} \quad (126)$$

Applying the property that  $\vartheta$  is unit vector along with simple calculations confirms equality  $\mathcal{K}^3 = -\mathcal{K}$ . This is sufficient to derive higher powers of  $\mathcal{K}$ , e.g. observe that  $\mathcal{K}^4 = \mathcal{K}\mathcal{K}^3 = -\mathcal{K}^2$  and so on. To proceed, let  $\kappa := (+1, -1, +1, \dots)$  be an alternating sign sequence, then for  $i = 1, 2, \dots$

$$\mathcal{K}^{2i-1} = \kappa_i \mathcal{K}, \quad \text{and} \quad \mathcal{K}^{2i} = \kappa_i \mathcal{K}^2 \quad (127)$$

Expanding  $\sin \alpha$  and  $\cos \alpha$  using Taylor series, then (122) turns to

$$\mathcal{R} = \mathbb{I} + \left(\alpha - \frac{\alpha^3}{3!} + \dots\right) \mathcal{K} + \left(\frac{\alpha^2}{2!} - \frac{\alpha^4}{4!} + \dots\right) \mathcal{K}^2 = \mathbb{I} + \alpha \mathcal{K} + \frac{\alpha^2}{2!} \mathcal{K}^2 - \frac{\alpha^3}{3!} \mathcal{K} - \frac{\alpha^4}{4!} \mathcal{K}^2 + \dots \quad (128)$$

Finally, replacing  $\mathcal{K}$  and  $\mathcal{K}^2$  by characterizations in terms of  $\mathcal{K}^{2i-1}$  and  $\mathcal{K}^{2i}$  stated in (127) in (128), then

$$\mathcal{R} = \mathbb{I} + \alpha \mathcal{K} + \frac{\alpha^2}{2!} \mathcal{K}^2 + \frac{\alpha^3}{3!} \underbrace{(-\mathcal{K})}_{\mathcal{K}^3} + \frac{\alpha^4}{4!} \underbrace{(-\mathcal{K}^2)}_{\mathcal{K}^4} + \dots = \sum_{n \geq 0} \frac{(\alpha \mathcal{K})^n}{n!} = \exp(\alpha \mathcal{K}) \quad (129)$$

The proof is complete by setting  $\Omega = \alpha \mathcal{K}$ .  $\square$

## APPENDIX B. TANGENT PLANE FOR DEFORMED PLANAR FRAME

**Proof of Lemma 4.3.** Following remark 4.4, we assume degree of internal vertex satisfies  $n \geq 3$ . We first show the claim on equivalency of (60) and the condition that all vectors  $\{\vec{i}_e(\mathbf{v})\}_{e \sim \mathbf{v}}$  lie in the same plane, i.e.  $(\vec{i}_1(\mathbf{v}) \times \vec{i}_2(\mathbf{v})) \cdot \vec{i}_e(\mathbf{v}) = 0$  for all  $e \sim \mathbf{v}$ . Setting  $w'_e = 0$  in the representation of  $\vec{i}_e(\mathbf{v})$  in (25), then

$$\left(\vec{i}_1(\mathbf{v}) \times \vec{i}_2(\mathbf{v})\right) \cdot \vec{i}_e(\mathbf{v}) = \left((\vec{i}_1 + v'_1 \vec{k}) \times (\vec{i}_2 + v'_2 \vec{k})\right) \cdot (\vec{i}_e + v'_e \vec{k}) \quad (130)$$

Applying properties  $(\vec{i}_1 \times \vec{i}_2) \cdot \vec{i}_e = 0$ ,  $(\vec{i}_1 \times \vec{k}) \cdot \vec{k} = 0$ , and  $(\vec{k} \times \vec{i}_2) \cdot \vec{k} = 0$  implies that

$$\left(\vec{i}_1(\mathbf{v}) \times \vec{i}_2(\mathbf{v})\right) \cdot \vec{i}_e(\mathbf{v}) = v'_1 \underbrace{(\vec{k} \times \vec{i}_2)}_{\vec{j}_2} \cdot \vec{i}_e + v'_2 \underbrace{(\vec{i}_1 \times \vec{k})}_{-\vec{j}_1 \cdot \vec{i}_e = \vec{j}_e \cdot \vec{i}_1} \cdot \vec{i}_e + v'_e \underbrace{(\vec{i}_1 \times \vec{i}_2) \cdot \vec{k}}_{\vec{i}_2 \cdot (\vec{k} \times \vec{i}_1) = \vec{i}_2 \cdot \vec{j}_1} \quad (131)$$

which is condition (60) as it has been claimed. Next we proceed with the proof of the Lemma. Firstly, in order to show (55b)  $\Rightarrow$  (60), observe that from (55b) and for  $e = 1, 2, \dots, n$  adjacent to the internal vertex

$$\vec{j}_e \cdot (\eta_1 \vec{i}_1 - v'_1 \vec{j}_1) = \vec{j}_e \cdot (\eta_e \vec{i}_e - v'_e \vec{i}_e) \quad \Rightarrow \quad (\vec{j}_e \cdot \vec{j}_1) v'_1 - (\vec{j}_e \cdot \vec{i}_1) \eta_1 - v'_e = 0$$

This then implies that the following linear system

$$\begin{pmatrix} 1 & 0 & v'_1 \\ \vec{j}_2 \cdot \vec{j}_1 & \vec{j}_2 \cdot \vec{i}_1 & v'_2 \\ \vec{j}_e \cdot \vec{j}_1 & \vec{j}_e \cdot \vec{i}_1 & v'_e \end{pmatrix} \begin{pmatrix} +v'_1 \\ -\eta_1 \\ -1 \end{pmatrix} = \begin{pmatrix} 0 \\ 0 \\ 0 \end{pmatrix}$$

holds. This implies that the multiplication matrix is rank deficient and thereby

$$(\vec{j}_2 \cdot \vec{i}_1)(\vec{j}_e \cdot \vec{j}_1) v'_1 - (\vec{j}_2 \cdot \vec{j}_1)(\vec{j}_e \cdot \vec{i}_1) v'_1 + (\vec{j}_e \cdot \vec{i}_1) v'_2 + (\vec{j}_1 \cdot \vec{i}_2) v'_e = 0 \quad (132)$$

Above we use the relation  $\vec{j}_2 \cdot \vec{i}_1 = -\vec{j}_1 \cdot \vec{i}_2$ . It remains to show that  $v'_1$  has the right multiplication coefficient, namely  $\vec{j}_2 \cdot \vec{i}_s$ . But

$$(\vec{j}_2 \cdot \vec{i}_1) \underbrace{(\vec{j}_e \cdot \vec{j}_1)}_{(\vec{i}_e \cdot \vec{i}_1)} - (\vec{j}_2 \cdot \vec{j}_1) \underbrace{(\vec{j}_e \cdot \vec{i}_1)}_{-(\vec{i}_e \cdot \vec{j}_1)} = \vec{j}_2 \cdot \underbrace{((\vec{i}_e \cdot \vec{i}_1) \vec{i}_1 + (\vec{i}_e \cdot \vec{j}_1) \vec{j}_1)}_{\vec{i}_e} = \vec{j}_2 \cdot \vec{i}_e$$

which proves (60). Secondly, to show that (55b)  $\Rightarrow$  (61), notice

$$\begin{aligned} \vec{j}_1 \cdot (\eta_1 \vec{i}_1 - v'_1 \vec{j}_1) &= \vec{j}_1 \cdot (\eta_e \vec{i}_e - v'_e \vec{i}_e) \quad \Rightarrow \quad (\vec{j}_1 \cdot \vec{j}_e) v'_e - (\vec{j}_1 \cdot \vec{i}_e) \eta_e - v'_1 = 0 \\ \vec{j}_2 \cdot (\eta_2 \vec{i}_2 - v'_2 \vec{j}_2) &= \vec{j}_2 \cdot (\eta_e \vec{i}_e - v'_e \vec{j}_e) \quad \Rightarrow \quad (\vec{j}_2 \cdot \vec{j}_e) v'_e - (\vec{j}_2 \cdot \vec{i}_e) \eta_e - v'_2 = 0 \end{aligned} \quad (133)$$

Similar argument on rank deficiency of coefficient matrix shows that

$$(\vec{j}_2 \cdot \vec{j}_e) v'_1 - (\vec{j}_e \cdot \vec{j}_1) v'_2 + (\vec{j}_1 \cdot \vec{i}_e)(\vec{j}_2 \cdot \vec{j}_e) \eta_e - (\vec{j}_1 \cdot \vec{j}_e)(\vec{j}_2 \cdot \vec{i}_e) \eta_e = 0$$

holds. But

$$(\vec{j}_1 \cdot \vec{i}_e)(\vec{j}_2 \cdot \vec{j}_e) - (\vec{j}_1 \cdot \vec{j}_e)(\vec{j}_2 \cdot \vec{i}_e) = \vec{j}_1 \cdot ((\vec{i}_2 \cdot \vec{i}_e) \vec{i}_e + (\vec{i}_2 \cdot \vec{j}_e) \vec{j}_e) = \vec{j}_1 \cdot \vec{i}_2 \quad (134)$$

Compare with (61), this finishes the desired result. Finally, it remains to show the reverse equality, i.e. (60) & (61)  $\Rightarrow$  (55b). Starting with (60)

$$(\vec{j}_1 \cdot \vec{i}_2) v'_e = -(\vec{j}_2 \cdot \vec{i}_e) v'_1 - (\vec{j}_e \cdot \vec{i}_1) v'_2 = \vec{j}_e \cdot (v'_1 \vec{i}_2 - v'_2 \vec{i}_1) \quad (135)$$

Similarly from (61),

$$(\vec{j}_1 \cdot \vec{i}_2) \eta_e = -(\vec{j}_2 \cdot \vec{j}_e) v'_1 + (\vec{j}_e \cdot \vec{j}_1) v'_2 = \vec{i}_e \cdot (v'_2 \vec{i}_1 - v'_1 \vec{i}_2) \quad (136)$$

This then implies that (assuming  $\vec{j}_1 \cdot \vec{i}_2 \neq 0$ )

$$\eta_e \vec{i}_e - v'_e \vec{j}_e = \frac{v'_2}{(\vec{j}_1 \cdot \vec{i}_2)} \vec{i}_1 - \frac{v'_1}{(\vec{j}_1 \cdot \vec{i}_2)} \vec{i}_2 \quad (137)$$

holds for all  $e \sim \mathbf{v}$ . Since the right hand side of (137) is independent of  $e$ , then the result in (55b) is clear.  $\square$

## REFERENCES

- [1] M. Arioli and M. Benzi. A finite element method for quantum graphs. *IMA Journal of Numerical Analysis*, 38:1119–1163, 2017.
- [2] R. Band, G. Berkolaiko, C. H. Joyner, and W. Liu. Quotients of finite-dimensional operators by symmetry representations. preprint [arXiv:1711.00918](https://arxiv.org/abs/1711.00918), 2017.
- [3] J. R. Banerjee. Review of the dynamic stiffness method for free-vibration analysis of beams. *Transportation Safety and Environment*, 1:106–116, 2019.
- [4] G. Berkolaiko, J. B. Kennedy, P. Kurasov, and D. Mugnolo. Surgery principles for the spectral analysis of quantum graphs. *Trans. Amer. Math. Soc.*, 372(7):5153–5197, 2019.
- [5] G. Berkolaiko and P. Kuchment. *Introduction to Quantum Graphs*, volume 186 of *Mathematical Surveys and Monographs*. AMS, 2013.
- [6] G. Berkolaiko, Y. Latushkin, and S. Sukhtaiev. Limits of quantum graph operators with shrinking edges. *Adv. Math.*, 352:632–669, 2019.
- [7] A. V. Borovskikh and K. P. Lazarev. Fourth-order differential equations on geometric graphs. *Journal of Mathematical Sciences*, 119:719–738, 2004.
- [8] V. I. Burenkov. *Sobolev spaces on domains*, volume 137 of *Teubner Texts in Mathematics*. B. G. Teubner, Stuttgart, 1998.
- [9] C. Castro and E. Zuazua. Boundary controllability of a hybrid system consisting in two flexible beams connected by a point mass. *SIAM Journal on Control and Optimization*, 36:1576–1595, 1998.
- [10] C. Castro and E. Zuazua. Exact boundary controllability of two Euler–Bernoulli beams connected by a point mass. *Mathematical and Computer Modeling*, 32:955–969, 2000.
- [11] K. L. Chan and F. W. Williams. Orthogonality of modes of structures when using the exact transcendental stiffness matrix method. *Shock and Vibration*, 7:653919, 2000.
- [12] B. Dekoninck and S. Nicaise. The eigenvalue problem for networks of beams. *Linear Algebra and its Applications*, 314(1-3):165–189, 2000.
- [13] H. L. Dret. Modeling of the junction between two rods. *Journal de Mathématiques Pures et Appliquées*, 68:365–397, 1989.
- [14] M. Etehad and B. Hatinoğlu. On the spectra of periodic elastic beam lattices: single layer graph. preprint [arXiv:2110.05466](https://arxiv.org/abs/2110.05466), 2021.
- [15] W. Fulton and J. Harris. *Representation theory*, volume 129 of *Graduate Texts in Mathematics*. Springer-Verlag, New York, 1991.
- [16] M. Geradin and D. J. Rixen. *Mechanical vibrations: theory and application to structural dynamics*. Wiley; 3rd edition, Feb. 2015.
- [17] F. Gregorio and D. Mugnolo. Bi-Laplacians on graphs and networks. *Journal of Evolution Equations*, 20(11):191–232, 2020.
- [18] D. Grieser. Thin tubes in mathematical physics, global analysis and spectral geometry. In *Analysis on graphs and its applications*, volume 77 of *Proc. Sympos. Pure Math.*, pages 565–593. Amer. Math. Soc., Providence, RI, 2008.
- [19] R. O. Grossi and C. M. Albarracín. Variational approach to vibrations of frames with inclined members. *Applied Acoustics*, 74:325–334, 2013.
- [20] Q. Gu, G. Leugering, and T. Li. Exact boundary controllability on a tree-like network of nonlinear planar timoshenko beams. *Chinese Annals of Mathematics, Series B*, 38(6):711–740, May 2017.
- [21] I. A. Karnovskii and O. I. Lebed. *Free vibrations of beams and frames : eigenvalues and eigenfunctions*. McGraw-Hill, New York, 2004.
- [22] T. Kato. *Perturbation theory for linear operators*. Classics in Mathematics. Springer-Verlag, Berlin, 1995. Reprint of the 1980 edition.
- [23] J.-C. Kiik, P. Kurasov, and M. Usman. On vertex conditions for elastic systems. *Physics Letters A*, 379(34-35):1871–1876, Sept. 2015.
- [24] T. Kottos and U. Smilansky. Periodic orbit theory and spectral statistics for quantum graphs. *Ann. Physics*, 274(1):76–124, 1999.
- [25] P. Kuchment. An overview of periodic elliptic operators. *Bull. Amer. Math. Soc. (N.S.)*, 53(3):343–414, 2016.
- [26] P. Kuchment and H. Zeng. Convergence of spectra of mesoscopic systems collapsing onto a graph. *J. Math. Anal. Appl.*, 258(2):671–700, 2001.
- [27] P. Kurasov. On the ground state for quantum graphs. *Lett. Math. Phys.*, 109(11):2491–2512, 2019.

- [28] P. Kurasov and J. Muller.  $n$ -Laplacians on metric graphs and almost periodic functions: I. *Annales Henri Poincaré*, 22:121–169, 2021.
- [29] J. E. Lagnese, G. Leugering, and E. J. P. G. Schmidt. Modelling and controllability of networks of thin beams. *System Modelling and Optimization. Lecture Notes in Control and Information Sciences*, 180:467–480, 1992.
- [30] J. E. Lagnese, G. Leugering, and E. J. P. G. Schmidt. *Modeling, analysis and control of dynamic elastic multi-link structures*. Systems & Control: Foundations & Applications. Birkhäuser Boston Inc., Boston, MA, 1994.
- [31] J. E. Lagnese, G. Leugering, and P. G. Schmidt. Modelling of dynamic networks of thin thermoelastic beams. *Mathematical Methods in the Applied Sciences*, 16:327–358, 1993.
- [32] G. Leugering, S. A. Nazarov, and A. S. Slutskiĭ. The asymptotic analysis of a junction of two elastic beams. *ZAMM - Journal of Applied Mathematics and Mechanics*, 99:1–22, 2019.
- [33] G. Leugering, S. A. Nazarov, A. S. Slutskiĭ, and J. Taskinen. Asymptotic analysis of a bit brace shaped junction of thin rods. *ZAMM - Journal of Applied Mathematics and Mechanics*, 99:1–11, 2019.
- [34] G. W. Mackey. *Unitary group representations in physics, probability, and number theory*, volume 55 of *Mathematics Lecture Note Series*. Benjamin/Cummings, Reading, Mass., 1978.
- [35] F. Mehmeti, J. V. Below, and S. Nicaise. *Partial differential equations on multistructures*. Marcel Dekker, Inc, 2001.
- [36] C. Mei. Wave analysis of in-plane vibrations of L-shaped and portal planar frame structures. *Journal of Vibration and Acoustics*, 134(2), 01 2012.
- [37] C. Mei. Analysis of in- and out-of plane vibrations in a rectangular frame based on two- and three-dimensional structural models. *Journal of Sound and Vibration*, 440(3):412–438, Feb. 2019.
- [38] C. Mei and R. Mace. Wave reflection and transmission in timoshenko beams and wave analysis of timoshenko beam structures. *Journal of Sound and Vibration*, 127(4):382–394, Aug. 2005.
- [39] G. P. Menzala, A. F. Pazoto, and E. Zuazua. Stabilization of Berger–Timoshenko’s equation as limit of the uniform stabilization of the von Kármán system of beams and plates. *Mathematical Modelling and Numerical Analysis*, 36:657–691, 2002.
- [40] D. Mercier and V. Régnier. Spectrum of a network of Euler–Bernoulli beams. *Journal of Mathematical Analysis and Applications*, 337:174–196, 2008.
- [41] D. Mugnolo, R. Nittka, and O. Olaf. Norm convergence of sectorial operators on varying Hilbert spaces. *Operators and Matrices*, 7:955–995, 2013.
- [42] H. P. Lin and J. Ro. Vibration analysis of planar serial-frame structures. *Journal of Sound and Vibration*, 262(15):1113–1131, May 2003.
- [43] O. Post. *Spectral Analysis on Graph-like Spaces*, volume 2039 of *Lecture Notes in Mathematics*. Springer Verlag, Berlin, 2012.
- [44] O. Post and J. Simmer. Quasi-unitary equivalence and generalized norm resolvent convergence. *Revue Roumaine des Mathématiques Pures et Appliquées*, 64:373–391, 2019.
- [45] A. R. Ratazzi, D. V. Bambill, and C. A. Rossit. Free vibrations of beam system structures with elastic boundary conditions and an internal elastic hinge. *Chinese Journal of Engineering*, pages 1–10, 2013.
- [46] K. Schmüdgen. *Unbounded self-adjoint operators on Hilbert space*, volume 265 of *Graduate Texts in Mathematics*. Springer, Dordrecht, 2012.
- [47] G. Sweers. When is the first eigenfunction for the clamped plate equation of fixed sign? *Electronic Journal of Differential Equations*, 6:285–296., 2001.
- [48] A. Tomović, S. Šalinić, A. Obradović, A. Grbović, and M. Milovančević. Closed-form solution for the free axial-bending vibration problem of structures composed of rigid bodies and elastic beam segments. *Applied Mathematical Modelling*, 77:1148–1167, 2020.
- [49] J. von Below. A characteristic equation associated to an eigenvalue problem on  $c^2$ -networks. *Linear Algebra Appl.*, 71:309–325, 1985.
- [50] F. W. Williams and W. H. Wittrick. An automatic computational procedure for calculating natural frequencies of skeletal structures. *Int. J. Mech. Sci.*, 12(9):781–791, 1970.
- [51] W. H. Wittrick and F. W. Williams. A general algorithm for computing natural frequencies of elastic structures. *Quart. J. Mech. Appl. Math.*, 24:263–284, 1971.
- [52] J. Ye. *Structural and Stress Analysis: Theories, Tutorials and Examples*. CRC Press, 2nd edition, 2015.
- [53] V. V. Zhikov. Homogenization of elasticity problems on singular structures. *Izvestiya: Mathematics*, 66:299–365, 2002.



- [54] V. V. Zhikov and S. E. Pastukhova. Bloch principle for elliptic differential operators with periodic coefficients. *Russian Journal of Mathematical Physics*, 23:257–277, 2016.

DEPARTMENT OF MATHEMATICS, TEXAS A&M UNIVERSITY, COLLEGE STATION, TX 77843-3368, USA

INSTITUTE FOR MATHEMATICS AND ITS APPLICATIONS (IMA), UNIVERSITY OF MINNESOTA, MINNEAPOLIS, MN 55455, USA